UNIVERSITAT POLITÈCNICA DE VALÈNCIA

UNIVERSITAT POLITÈCNICA DE VALÈNCIA

Dept. of Biotechnology

Exploring Activator Protein-1s (AP-1) journey across the cell cycle of cancer cells

Master's Thesis

Master's Degree in Biomedical Biotechnology

AUTHOR: Antón Salvador, Javier

Tutor: Galindo Orozco, Máximo Ibo

External cotutor: Farràs Rivera, Rosa

Experimental director: Gandía Ventura, Carolina

ACADEMIC YEAR: 2023/2024

Title (English): Exploring Activator Protein-1's (AP-1) journey across the cell cycle of cancer cells.

Abstract (English): Cancer is a heterogeneous group of diseases with increasing incidence and expected to be the first global cause of death in the 21st century. Lung cancer is the most common type of cancer, being NSCLC the most common lung cancer subtype, and the one our group is mainly focused on. AP-1 was one of the first mammalian transcription factors discovered, being composed of dimers formed from the Jun and Fos subfamilies, among others. AP-1 has a complex role in several diseases, including cancer, participating in oncogenic transformation, cell proliferation, apoptosis, and progression through the cell cycle. Fra2 is the most recently identified member of AP-1, and its concrete role in carcinogenesis is largely uncharacterized, even though evidence suggests implication in cell proliferation, transformation, and cell cycle control.

The goal of the present study is to characterize patterns of expression of AP-1 (Jun and Fos) members, and especially Fra2, across the cell cycle at the protein and mRNA level, infer possible regulation mechanisms and broaden the knowledge of AP-1's implication in the cell cycle of cancer cells.

Towards this goal, U2OS osteosarcoma cells were synchronized using double thymidine blockage, with following analysis of total genomic content variation, using flow cytometry, protein expression variation of AP-1 and representative cyclins using Western Blot, and mRNA expression variation of AP-1 using RT-qPCR. Drastically different expression patterns were obtained for different AP-1 (Jun and Fos) members, which relate to their different roles at diverse stages of the cell cycle of cancer cells.

In conclusion, the present study allowed the characterization of AP-1 (Jun and Fos) across the cell cycle of cancer cells and will serve as a basis for future studies.

Keywords (English): AP-1 | Cell Cycle | Flow Cytometry | Fos | *FOSL2* | Fra2 | Jun | Lung Cancer | NSCLC | Osteosarcoma | RT-qPCR | Thymidine | Transcription Factor | U2OS | Western Blot

Título (Castellano): Explorando el viaje de la Proteína Activadora-1 (AP-1) a lo largo del ciclo celular de células cancerosas.

Resumen (Castellano): El cáncer es un grupo heterogéneo de enfermedades cuya incidencia está en aumento y el cual se espera que constituya la principal causa de muerte del siglo XXI. El cáncer de pulmón es el tipo más frecuente de cáncer, siendo el CPNM el subtipo más habitual y en el cual el grupo se focaliza principalmente. AP-1 fue uno de los primeros factores de transcripción descubiertos en mamíferos, estando compuesto por dímeros de miembros de las familias Jun y Fos, entre otros. AP-1 participa de forma compleja en diferentes enfermedades, incluyendo el cáncer, en el que tiene un papel en la transformación oncogénica, la proliferación celular, la apoptosis y la progresión a lo largo del ciclo celular. Fra2 es el último miembro de AP-1 en ser identificado, y su función concreta en la carcinogénesis aún está por caracterizar, si bien existe evidencia que apunta a una implicación en la proliferación y transformación celular, así como en el control del ciclo celular.

El objetivo del presente trabajo es caracterizar los patrones de expresión de miembros de AP-1 (Jun y Fos), y, especialmente Fra2, a lo largo del ciclo celular, tanto a nivel de proteína como de ARNm, inferir posibles mecanismos de regulación y ampliar el conocimiento sobre la implicación de AP-1 en el control del ciclo celular de las células cancerosas.

Con este objetivo, se sincronizaron células U2OS de osteosarcoma utilizando bloqueo por doble timidina, con posterior análisis del contenido genómico total, usando citometría de flujo, de la variación en expresión proteica de AP-1 usando Western Blot, y de la variación en expresión de ARNm de AP-1 usando RT-qPCR. Se observaron patrones de expresión drásticamente distintos para los distintos miembros de AP-1 (Jun y Fos), que se relacionan con sus distintas funciones a lo largo de las diversas fases del ciclo celular en células cancerosas.

Como conclusión, el presente estudio permitió la caracterización de AP-1 (Jun y Fos) a lo largo del ciclo celular de células cancerosas, sirviendo como base para futuros estudios.

Palabras Clave (Castellano): AP-1 | Cáncer de Pulmón | Ciclo Celular | Citometría de Flujo | Factor de Transcripción | Fos | *FOSL2* | Fra2 | Jun | Osteosarcoma | RT-qPCR | Timidina | U2OS | Western Blot

Abbreviations

- *AA:BAA:* Acrylamide:Bisacrylamide
- *AECC:* Asociación española contra el cáncer
- *ALK:* Anaplastic lymphoma kinase
- *ANOVA:* Analysis of variance
- *AP-1:* Activator protein-1
- *APS:* Ammonium persulfate
- *ATCC:* American Type Culture Collection
- *BCA:* Bicinchoninic acid assay
- *bZIP:* Basic-region leucine zipper
- *CAF:* Cancer-associated fibroblast
- *cAMP:* Cyclic adenosyl monophosphate
- *CDK:* Cyclin-dependent kinase
- *cDNA:* Complementary DNA
- *ChIP:* Chromatin immunoprecipitation
- *CIPF:* Centro de Investigación Príncipe Felipe
- *CoIP:* Co-immunoprecipitation
- *CRE:* cAMP-response element
- *DMEM:* Dulbecco Modified Eagle's Medium
- *DNA:* Desoxyribonucleic acid
- *dPCR:* Digital PCR
- *ECM:* Extracellular matrix
- *EGFR:* Epidermal growth factor receptor
- *ELISA:* Enzyme-linked immunosorbant assay
- *ERK:* Extracellular-regulated kinase
- *FBS:* Fetal bovine serum
- *FDA:* Food & drug administration
- *FRA1:* Fos-related antigen 1
- *FRA2:* Fos-related antigen 2
- *GFP:* Green fluorescent protein
- *GUSB:* Glucuronidase beta
- *HRP:* Horse radish peroxidase
- *IRES:* Internal ribosomal entry site

- *JNK:* c-Jun N-terminal kinase
- *KRAS:* Kirsten rat sarcoma viral oncogene homolog
- *LHRH:* Luteinizing hormone-releasing hormone
- *lncRNA:* Long non-coding RNA
- *MAPK:* Mitogen activated protein kinase
- *MEF2C:* Monocyte-specific enhancer binding factor 2c
- *MS:* Mass spectrometry
- *NK:* Natural killer
- *NSCLC:* Non-small cell lung carcinoma
- *PAGE:* Polyacrylamide gel electrophoresis
- *PBS:* Phosphate buffer saline
- *PVDF:* Polyvinylidene difluoride
- *qRT-PCR:* Quantitative reverse transcription polymerase chain reaction
- *RNA:* Ribonucleic acid
- *RPS26:* Ribosomal protein S26
- *SDS:* Sodium dodecyl sulphate
- *siRNA:* Silencing RNA
- *TAM:* Tumor-associated macrophage
- *TCF:* Ternary complex factor
- *TEMED:* Tetramethylethylenediamine
- *TKI:* Tyrosine kinase inhibitor
- *TME:* Tumor microenvironment
- *TPA:* 12-O-tetradecanoylphorbol 13-acetate
- *TRE:* TPA-response element
- *UPV:* Universidad politécnica de Valencia
- *WB:* Western blot

Acknowledgements

Firstly, I want to thank Rosa for giving me the opportunity of being a part of the group and allowing me to engage hands-on with science. I want to thank her for trusting me, for giving me guidance and for listening to my concerns along the way.

I want to thank the Spanish Association Against Cancer (AECC) for providing me the essential funding needed to sustain me during the time in the lab this past year, and during the remaining years of my PhD.

I want to thank Carol for teaching me most of what I know about lab work, and especially helping me in this project, which has been crucial for me regarding finishing this work and all the experimental replicates within it.

I want to thank my colleagues in the lab, especially Juanfran, for being there during much of the process, accompanying me through some of the toughest days and being able to talk about our common problems, concerns and the overwhelming stress that can come from lab work.

I want to thank my friends, for giving me those little moments that allowed me to disconnect, step back and look from a different perspective, knowing we share many problems, and we may all eventually find a way to solve them.

I want to thank my family, my parents and sisters, which have been the backbone of the support network I've had during these months and have always helped me to get over all the bumps along the way, not only now, but always.

Finally, I want to thank Patri, as she has been insanely important in keeping me afloat in the darkest moments, in helping me deal with stress and with impostor syndrome, and at the same time has provided me with some of the best and happiest moments certainly of the past year, and for most of my life. Thank you for your intelligent advice, your kindness and patience.

Index

Figure Index

Table Index

Introduction

Cancer, an increasingly complex disease

Cancer represents a heterogeneous group of diseases that present some common characteristics that have come to constitute "The Hallmarks of Cancer" *(Figure 1A)*. These represent some properties that most human cells acquire during the process of neoplastic transformation and include the ability to sustain proliferative signaling, evading growth suppressors, resisting cell death, enabling replicative immortality, inducing/accessing vasculature, activating invasion and metastasis, reprogramming cellular metabolism, and avoiding immune destruction. (Hanahan & Weinberg, 2011) These hallmarks have been properly stablished during the past decades and were later significantly expanded with the addition of enabling characteristics and emerging hallmarks. Enabling characteristics include those characteristics that would provide the means for cancer cells to acquire these hallmarks, including genomic instability and tumor-promoting inflammation. Several emerging hallmarks were also proposed and are being established as core hallmarks of cancer. These include the unlocking of phenotypic plasticity, the presence of non-mutational epigenetic reprogramming in cancer cells, the importance of polymorphic microbiomes in cancer and the relation between senescence and cancer onset. (Hanahan, 2022) Even though cancer hallmarks have been proven as a useful conceptual tool for understanding cancer as whole, below their simplicity underlies a complex diversity of mechanistic effects and phenotypes, both inside the tumor and system wide. Recently, different clouds of complexity have been proposed, the understanding of which is thought to be crucial for the improvement in cancer prevention and treatment. Some of these complexity clouds include neural-cancer crosstalk, cancer-induced cachexia, circadian clocks and cancer, thrombo-inflammation, and the relation of environmental factors such as dietary influences and physical activity with the disease. (Swanton et al., 2024)

Cancer is the first or second cause of death before age 70 in 91 of 172 countries, being third or fourth in an additional 22 countries. It is expected to rank as the leading cause of death globally, as well as the most important barrier for life expectancy increase in the 21st century. In both sexes combined, lung cancer is the most common diagnosed cancer, comprising 11,6 % of total cases, and the leading cause of death, with 18,4 % of total deaths. When taking sex into account, lung cancer represents the most common cancer among males, as well as the one with highest mortality. For females, lung cancer falls to third place regarding incidence, behind breast cancer and colorectal cancer, but second overall regarding mortality, only behind breast cancer *(Figure 1B)*. (Bray et al., 2018) Incidence and mortality data worldwide support the need for research in lung cancer and call as well for preventative measures.

The main etiological factor involved in lung carcinogenesis is tobacco consumption. In fact, the rise in lung cancer incidence among women that has been observed recently in countries such as Austria, Finland, Hungary, and the Netherlands, can be largely explained by the rising smoking rate among women in these countries *(Figure 1C)*. Other factors involved in lung cancer development are genetic susceptibility, poor diet, alcohol consumption, occupational exposures (Asbestos, metals, silica, polycyclic aromatic hydrocarbons…), and air pollution, which can act independently or

in addition to smoking. (Malhotra et al., 2016) Thus, despite lung cancer being heavily associated with different risk factors and mainly to smoking, and consequently being a largely preventable disease, it remains the type of cancer responsible of most overall deaths, and much work is still to be done regarding education, conscientization and prevention.

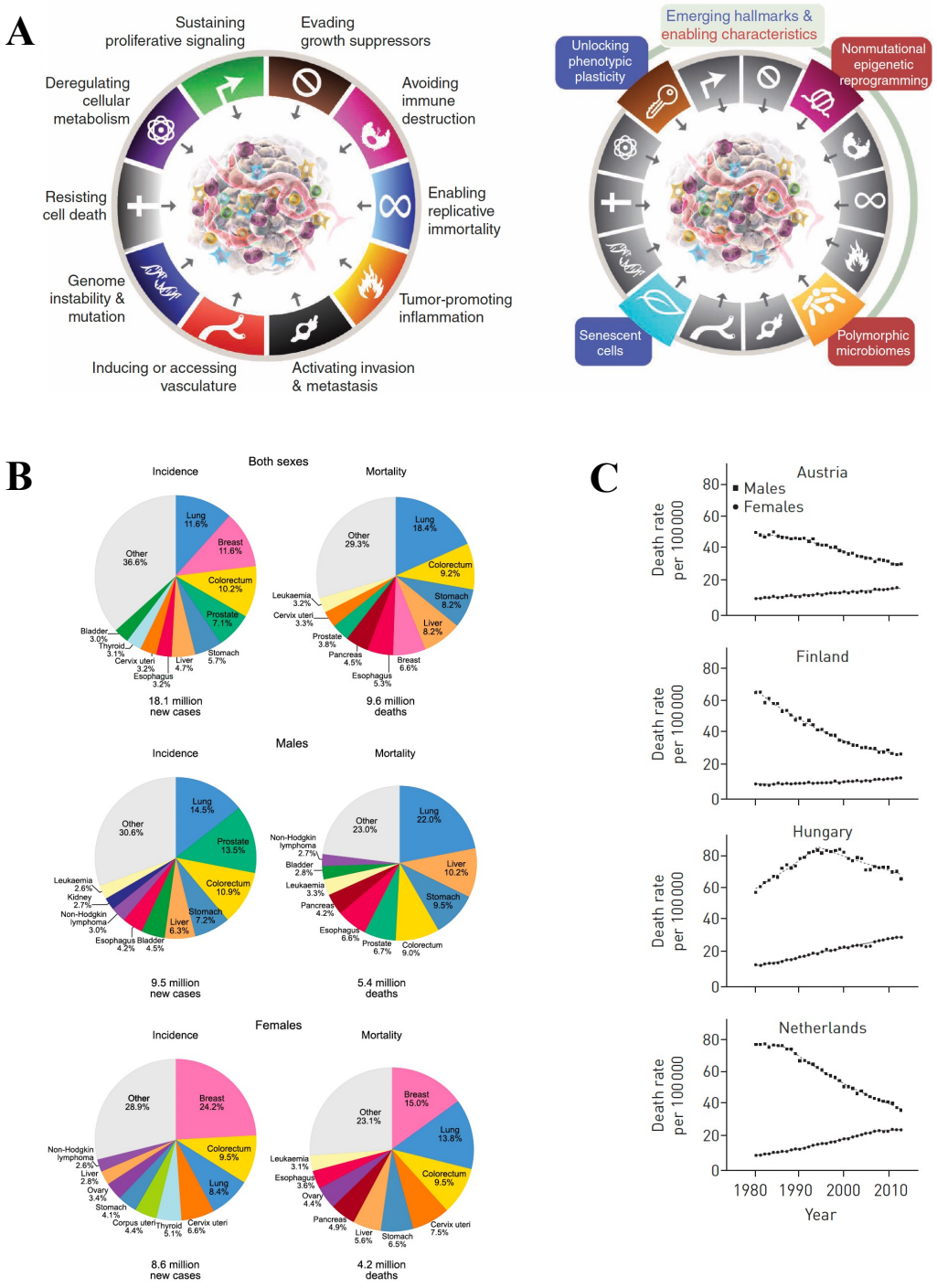

Figure 1. **Cancer hallmarks, incidence & mortality.** ***A.*** Hallmarks of cancer, including emerging hallmarks and enabling characteristics. Extracted from (Hanahan, 2022). ***B.*** Global incidence and mortality data for different types of cancer, either taking account or nor of patient sex, showing the importance of lung cancer research and prevention. Extracted from (Bray et al., 2018). ***C.*** Lung cancer

death rate in several countries from 1980 to 2018, split into sexes, showing growth in lung cancer deaths among women. Extracted from (Malhotra et al., 2016).

Lung cancer can be classified in different histological subtypes, including adenocarcinoma, squamous cell carcinoma, small-cell carcinoma, and large-cell carcinoma as the most common types. Adenocarcinoma, squamous cell carcinoma, and large-cell carcinoma are frequently grouped together to form a histologically heterogeneous group, non-small-cell lung cancer (NSCLC). Adenocarcinoma is the most common subtype of lung cancer, representing around 39 % of global cases, followed by squamous cell carcinoma, with 25 % of cases, small-cell carcinoma, with 11 %, and large-cell carcinoma, representing 8 % of global cases *(Figure 2A)*. The remaining 17 % of global cases are represented by less frequent types of lung cancer. This means that NSCLC represents collectively 72 % of global lung cancer cases, being by far the most frequent type of lung cancer and the one we primarily study in our lab. (Y. Zhang et al., 2023a) The principles for lung cancer classification are based on using morphology first, using support by immunohistochemistry (IHC), and then using molecular techniques if required. (Nicholson et al., 2022)

NSCLC cases are caused by acquired genetic alterations in certain driver genes, frequently those involved in proliferation and survival. The proto-oncogene that most frequently exhibits driver mutations in NSCLC is *KRAS*, with 29 % of cases, followed by *EGFR*, with 19 %, and less common mutations such as those involving *BRAF*, *MET*, *HER2* or *ALK* *(Figure 2B)*. (Chevallier et al., 2021) This oncogenic driver mutations represent potential druggable targets and are the basis for the development of targeted therapies, an important component of personalized medicine in lung cancer treatment.

Treatment of NSCLC in stages I or II is the surgical resection of the tumor, followed by adjuvant therapy to prevent cancer recurrence. However, when the disease reaches stages III or IV, recommended treatment changes to chemotherapy or radiotherapy. These treatments have known limitations, including non-specific targeting, and so abundant side-effects, as well as the development of drug resistance. To treat lung cancer, medicine has advanced in a more personalized manner and a myriad of different treatment strategies have emerged. This includes immunotherapy, based on the reactivation of the patients' immune system to attack tumor cells using, for example, checkpoint inhibitors, such as PD-1/PD-L1 inhibitors, oncolytic viruses, tumor vaccines or chimeric antigen receptor T (CAR-T) cell therapy among others. Further emergent strategies include nanodrug-based delivery systems, which improve drug efficacy and reduce off-target effects, and photodermal therapy, which uses local laser irradiation to generate heat that kills tumor cells, sometimes combined with nanotherapy. Non-invasive approaches such as liquid biopsy have also been revolutionary, as they can detect tumor recurrence, metastasis and follow treatment response without the need of a procedure such as tissue biopsy, and with astonishing precision. (L. Li et al., 2024)

Perhaps the most impactful of all has been the development of molecular targeted therapies, that is, drugs that specifically target mutations in certain oncogenes. Tyrosine kinase receptors, such as epidermal growth factor receptor (EGFR) and anaplastic lymphoma kinase (ALK) have been vital targets for targeted therapies. Tyrosine kinase inhibitors (TKIs) such as gefitinib, erlotinib or osimertinib have been greatly effective, even though acquired drug resistance is often inevitable, using different mechanisms including mutations, epigenetic alterations, or tumor subtype switching *(Figure 2C)*. It was previously mentioned that the most frequently mutated proto-oncogene in NSCLC

was Kirsten rat sarcoma viral oncogene homolog (KRAS), being *KRAS* ^{G12C} the most frequent mutation within it. Even though inhibitors for this mutation have been developed and FDA approved for their use, such as sotorasib and adagrasib, their efficacy has been modest and drug resistances have arisen, remarking the need for new therapeutic strategies and for a better understanding of oncogenic signaling in NSCLC. (Y. Li et al., 2023) (Rocco et al., 2016) (Carrera & Ormond, 2015) (Deb et al., 2022)

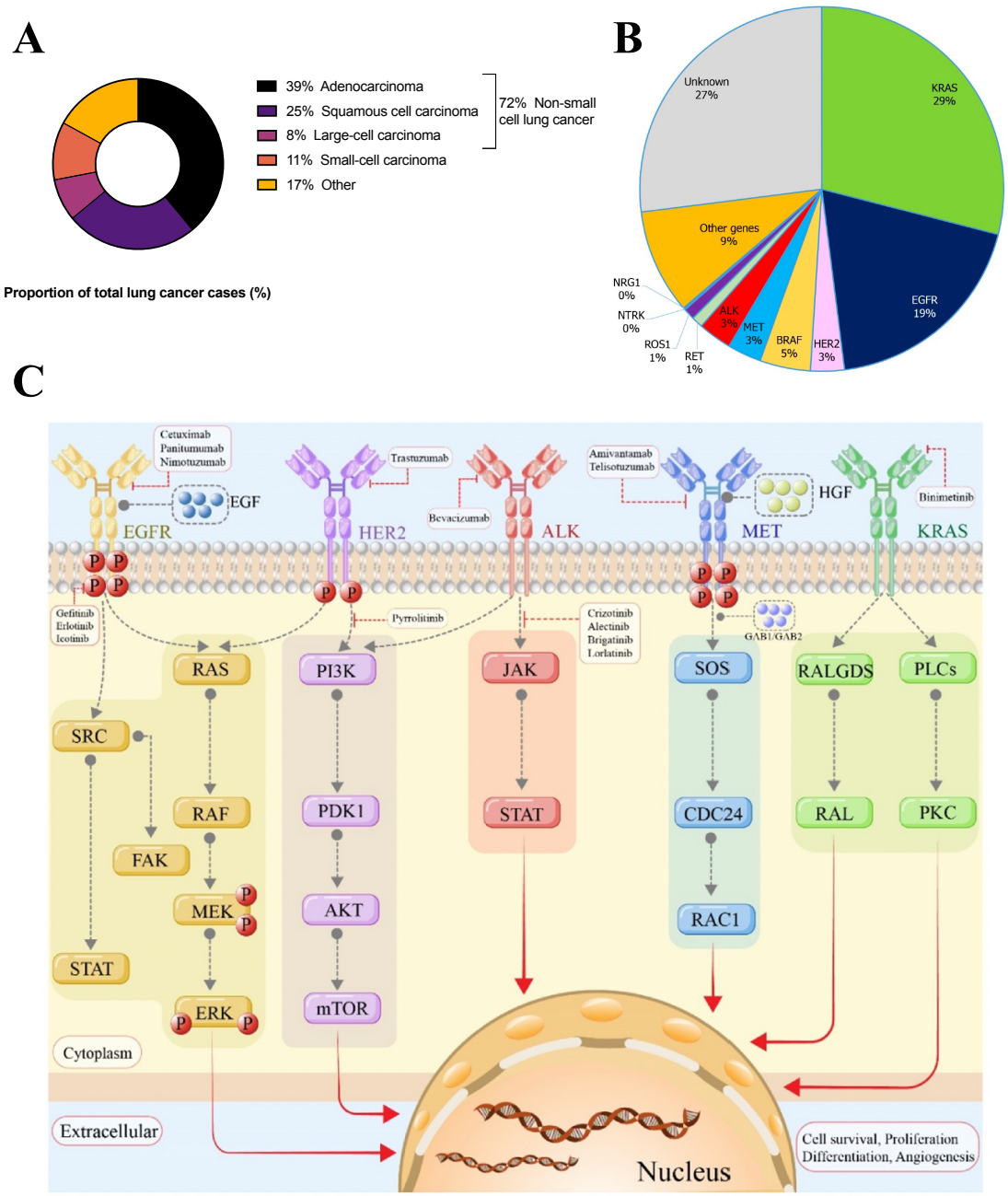

Figure 2. **Histological subtypes of lung cancer, oncogenic driver mutations & molecular targeted therapies.** ***A.*** Most frequent histological subtypes of lung cancer, as well as their global frequency. Data obtained from (Y. Zhang et al., 2023b), graphed using GraphPad Prism 9.5.0. ***B.*** Most frequent oncogenic driver mutated genes in NSCLC. Figure extracted from (Chevallier et al., 2021). ***C.*** Molecular targeted therapies and the signaling pathways affected by their inhibition. Figure extracted from (Y. Li et al., 2023).

Cell cycle and cell synchronization

The cell cycle is defined as the process that a cell undergoes driving it to division and the production of two daughter cells. The cell cycle is divided into G_1, S, G_2 and M, and progression through it is mediated by cyclin-dependent kinases (CDKs) and cyclins, their regulatory subunits. In the G_1 phase, cells grow larger. In the S phase, DNA replication takes place. In the G_2 phase DNA replication is assured and preparation for mitosis takes place. In the M phase, mitosis takes place, with chromosome segregation and cell division.

Different cell cycle checkpoints ensure that several processes have taken place before progressing to the next phase *(Figure 3)*. The three main ones are the G_1/S checkpoint, also known as the restriction (R) point, the G_2/M checkpoint, in which DNA integrity is checked, and the spindle assembly checkpoint (SAC), in which the alignment of the chromosomes at the metaphase plate is verified. In early G_1, cyclin D complexes with CDK4/6, driving the phosphorylation of retinoblastoma (Rb). This causes the release of transcription factor E2F, leading to the expression of different genes, including cyclins A and E. As G_1 progresses, binding of cyclin E and CDK2 produces full phosphorylation of Rb and the progression through the restriction point (G_1/S). As S phase is initiated, cyclin A is produced and subsequently binds to CDK2, driving DNA replication and G_2 progression. During late S phase, cyclin A binds to CDK1, contributing to the stabilization of cyclin B-CDK1. This complex increases along G_2 until it peaks, driving the transition to M phase, and is posteriorly degraded as mitosis comes to an end. Cyclin C's function is much more debated but seems to play a role in the transition from G_0 to G_1 by interacting with CDK3. (Martínez-Alonso & Malumbres, 2020)

To properly study and understand it, it is necessary to have a population of cells that transverse across the cell cycle in a synchronous way. With this intent, several protocols for cell synchronization have been developed. This includes methods that use chemical inhibitors and those that don't. Methods that don't use chemical inhibitors include serum starvation, which forces G_0 entry, contact inhibition, which blocks cells at early G_1, mitotic shake-off, in which mitotic cells are collected, FACS sorting and centrifugal elutriation, which can discern between G_1, S and G_2/M cells. These methods avoid the side effects associated to inhibitors but present a lesser yield and are less specific. (Davis et al., 2001) (Z. Wang, 2022) Methods that do use chemical inhibitors include G_1 phase synchronization by lovostatin, early S phase synchronization by double thymidine block, G_2 phase synchronization using CDK1 inhibitors, such as RO-3306 and Roscovitine, and M phase synchronization using Nocodazole, MG132, and Blebbistatin. Double thymidine block is based on the ability of high concentrations of thymidine to block ribonucleotide reductase enzymatic activity, responsible of converting ribonucleotides into deoxyribonucleotides. This reduces deoxyribonucleotide supply, causing the interruption of DNA synthesis. If only one thymidine treatment was performed, cells would be blocked at different stages of the S phase, and they would progress through the cell cycle in a heterogeneous matter after release. To obtain a homogeneous population at the start of the S phase, a second thymidine treatment is required, causing cells to stop as soon as they enter the S phase. (Pérez-Benavente & Farràs, 2016) Its main advantages over other synchronization methods are simplicity, as cell cycle release takes place just by washing thymidine off the media, and the low cost of the treatment itself. This method can, however, induce replication stress and cause imbalances in nucleotide pools. (Z. Wang, 2022) It is important to consider that when

performing cell synchronization using chemical inhibitors, the least interference is preferred, to reduce their side effects. In this way, double thymidine synchronization is easily the best method. (R. C. Wang & Wang, 2022)

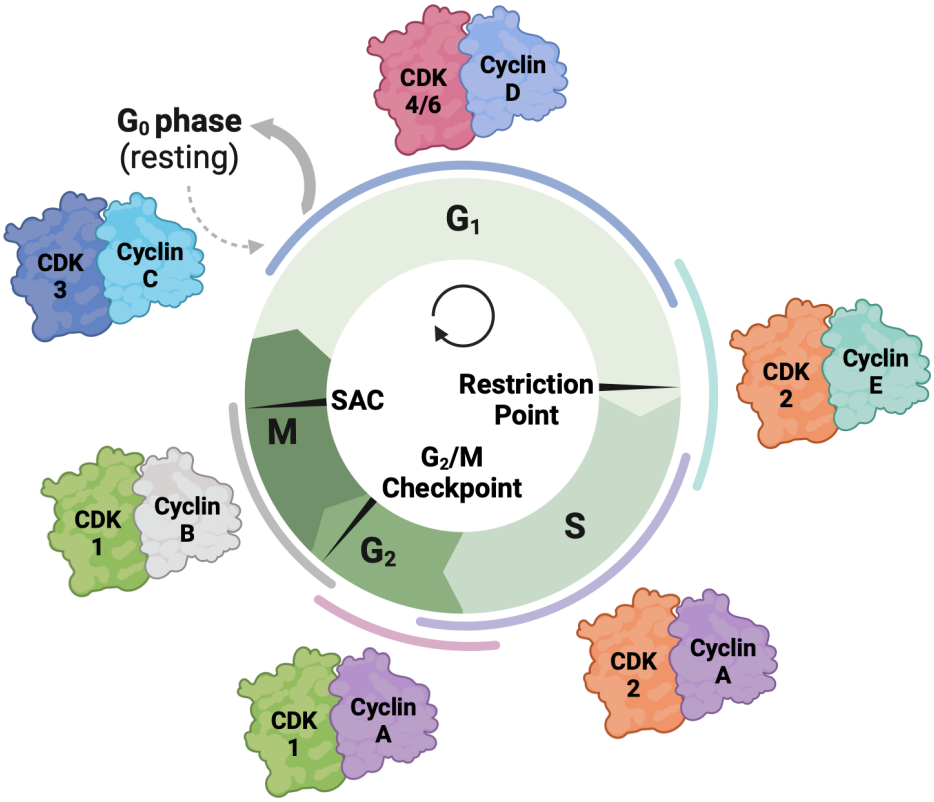

Figure 3. **Cell cycle, progression and regulation.** Progression across the cell cycle is regulated by the activity of CDKs and their corresponding cyclins. They regulate the progression across different checkpoints that ensure cell processes have taken place before continuing. Adapted from (Z. Wang, 2022). Constructed using BioRender.

Activator Protein-1 (AP-1), master signaling integrator

Activator Protein-1 (AP-1) was one of the first mammalian transcription factors identified. However, its specific functions and regulation are still largely unknown. (Eferl & Wagner, 2003) Firstly, it is important to know that AP-1 is not a single protein, but a collection of dimers formed from proteins from Jun and Fos subfamilies *(Figure 4A)*. These proteins present basic-region leucine zipper (bZIP) domains that allow their interaction with major groves in DNA *(Figure 4D)*. Specifically, AP-1 can recognize a particular DNA sequence, 5'-TGAG/CTCA-3', located at the promoter or enhancer regions of target genes. As its binding affinity can be enhanced by 12-O-tetradecanoylphorbol 13-acetate (TPA), its binding motif is denominated the TPA-response element (TRE). AP-1 composed of heterodimers from Jun and ATF can additionally bind to the DNA sequence, 5'-TGAGCGTCA-3', responding to cAMP and consequently receiving the denomination of cAMP-response elements (CRE). (Song et al., 2023)

The Jun subfamily is composed of three members; c-Jun (*JUN*), JunB (*JUNB*) and JunD (*JUND*); and can form the AP-1 transcription factor either by homodimerization of Jun proteins, or by heterodimerization with Fos members. The Fos subfamily is composed

of four members; c-Fos (*FOS*), FosB (*FOSB*), Fra1 (*FOSL1*) and Fra2 (*FOSL2*); and can form the AP-1 transcription factor only by heterodimerizing with Jun proteins. Regulation of AP-1 is complex and takes place at different levels; firstly, by altering the transcription of mRNAs of *jun* and *fos* families, as well as their turnover; secondly, by regulation of the stability of Jun and Fos proteins; thirdly, through post-translational modifications in Jun and Fos proteins that alter their function; and fourthly, through protein-protein interactions with other transcription factors that can either synergize or antagonize AP-1. It must be said that Fos:Jun heterodimers present stronger DNA-binding affinity, and stronger transcriptional stimulation than Jun:Jun dimers. (Halazonetis et al., 1988)

AP-1 activity is induced in response to a variety of stimuli *(Figure 4B)*, such as growth factors, neurotransmitters, cell-matrix interactions, peptide hormones, infections, and other kids of physical and chemical stresses. These different stimuli lead to the activation of mitogen activated protein kinase (MAPK) cascades. Growth factors mainly activate the extracellular-regulated kinase (ERK) subgroup of MAPKs, that can lead to the activation of AP-1 by phosphorylation of different targets. They can potentiate AP-1 transcription through activation of ternary complex factors (TCFs) that bind to *fos* promoters, and they can furthermore directly phosphorylate AP-1 members such as Fra1 and Fra2 to enhance their function. By contrast, genotoxic stress and pro-inflammatory cytokines mainly activate AP-1 through MAPK cascades involving p38 and c-Jun N-terminal kinases (JNKs). JNKs can translocate to the nucleus and directly phosphorylate c-Jun, increasing its transcriptional activity, and ATF2, binding partner to c-Jun. Additionally, p38 can contribute to AP-1 activation through direct phosphorylation of ATF2, TCFs and monocyte-specific enhancer binding factor 2c (MEF2C), which increases c-Jun expression. Other than the aforementioned stimuli, AP-1 activity can be elevated through constitutive expression of oncogenes, which cause the permanent activation of ERKs and JNKs. (Shaulian & Karin, 2002)

AP-1 is known to be involved in a variety of cellular and physiological processes, acting as a master integrator of different extracellular signals, and critically involved in the adaptations that cells undergo to changes in their environment *(Figure 4C)*. (Trop-Steinberg & Azar, 2017) AP-1 is implicated in different diseases, including transplant rejection, fibrosis, organ injury and inflammatory diseases such as asthma, psoriasis, and rheumatoid arthritis. (Motomura et al., 2018) The disease in which AP-1 has been most thoroughly studied, and the focus of the present work, is cancer, participating in cell transformation, tumor progression, aggressiveness, and resistance to treatments. (Trop-Steinberg & Azar, 2017) For this reason, AP-1 itself has become a drug target in precision oncology. Several small molecules targeting AP-1 are in clinical trials, either inhibiting AP-1 binding to DNA, such as T-5224, inhibiting JNK and so AP-1 phosphorylation, such as SP600125, and inhibiting dimerization of c-Jun, such as MLN944. (Kamide et al., 2016) (J. Wang et al., 2011) (Verborg et al., 2007) These drugs are promising mainly the enhancement of targeted therapies through combination therapy, as well as the reversal of drug AP-1-mediated resistance to other inhibitors. (Song et al., 2023) Even though AP-1 members are crucial in cancer pathophysiology, with certain exceptions, they rarely act as oncogenes or tumor suppressors on their own. Contrarily, they usually are downstream effectors of oncogenes, such as *KRAS*, *BRAF* or *EGFR*. (Bejjani et al., 2019)

It is known AP-1 plays a significant role in regulating apoptosis and cell survival. Apoptosis is a physiological process that suppresses oncogenic transformation and is essential for organogenesis and proper immune response. AP-1 contributes to apoptosis

both as an inducer and a repressor of the process. There are different models that explain its role in apoptosis, either suggesting that AP-1 activates both pro and anti-apoptotic genes whose balance determines cellular fate, or that AP-1 acts as a homeostatic regulator of cell survival, and constant and persistent activation or suppression can lead to changes in that balance. It is clear, however, that AP-1s role in apoptosis and cell survival is cell-specific and varies with stimulus type. (Shaulian & Karin, 2002)

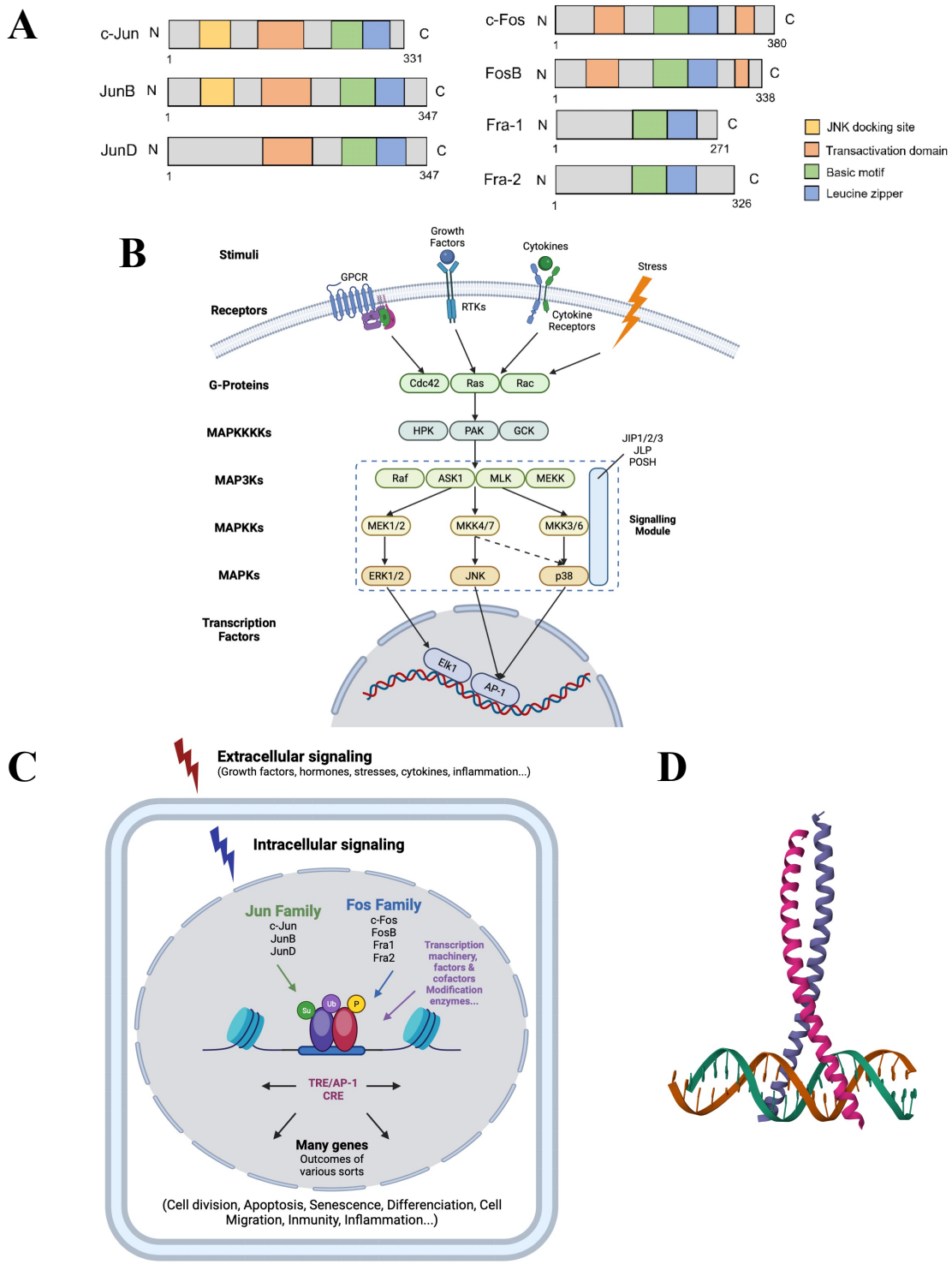

Figure 4. **AP-1 transcription factor; Jun and Fos subfamilies.** ***A.*** Jun and Fos AP-1 members, including their structural motifs. Figure extracted from (Song et al.,

2023). ***B.*** Signaling pathways leading to the activation of AP-1 transcription factors. Adapted from (Zhao et al., 2015). Constructed using BioRender. ***C.*** Differing cellular processes as outcomes of AP-1 activation. Adapted from (Bejjani et al., 2019). Constructed using BioRender. ***D.*** Crystal structure of the leucine zipper domain present in the heterodimeric c-Fos:c-Jun transcription factor bound to DNA. Structure obtained from Protein Data Bank, uploaded from (Glover & Harrison, 1995).

As it was already mentioned, AP-1 plays a role in oncogenic transformation and cell proliferation. This role is far more complex that it was previously thought, in some instances seemingly contradictory and highly tissue dependent. It has been thoroughly proved, however, that some AP-1 members are required for cell proliferation and cell cycle progression. (Shaulian & Karin, 2002) Significant correlations have been observed between protein expression of AP-1 members and that of different cell cycle promoters (Cyclin E, Cyclin B1, Cyclin D1, CDK2 and CDK4) and inhibitors (Rb, p16, p21). As the expression of a particular AP-1 member can be both correlated with the expression of cyclins and cell cycle inhibitors, it is thought that cell cycle progression in certain types of cancer is regulated by relative abundance of AP-1 members. (Bamberger et al., 2001) Some AP-1 members have been discovered as direct regulators of different cyclins. c-Jun promotes cyclin D1 expression in G_1, and JunB is a repressor of cyclin D1 and an inducer of p16. (Bakiri et al., 2000) (Passegué & Wagner, 2000) JunB and Fra1 act as inducers of cyclin A2 expression, and JunB degradation during mid/late G_2 is key in the downregulation of this cyclin during prometaphase. (Andrecht et al., 2002) (Casalino et al., 2007) Aberrant expression of JunB during this phase can consequently lead to genomic instability and play a role in tumorigenesis. (Farràs et al., 2008) Furthermore, JunB can also induce the expression of cyclin E1, and its over-expression correlated with poor prognosis in breast and ovarian cancer. (Pérez-Benavente et al., 2022)

Fos-related antigen-2 (Fra2): AP-1's newest member

The most recently discovered member of AP-1 is fos-related antigen-2 (Fra2), codified by the *FOSL2* gene. As previously stated, Fra2 is a member of the Fos subfamily, and even though there is significant similarity between the different Fos members, it is relevant to remark both Fra1 and Fra2 lack the C-terminal transactivation domain present in c-Fos and FosB *(Figure 4A and 5A)*. Even though significant evidence of Fra2 implication in cancer has been collected in the past three decades since its discovery, its specific role is still yet to be understood, and evidence varies widely depending on neoplasm type. Furthermore, Fra2 function regulation, as well as other AP-1 members, is extremely complicated *(Figure 5B)*, involving diverse signaling pathways and miRNAs. Once Fra2 is activated, different dimers can be formed with each Jun member, which in turn translates into different DNA-binding sites and targets, being able to either activate or repress gene expression. Subsequently, Fra2 takes part in biological processes in a seemingly contradictory manner, being a regulator of cell survival and cell death, differentiation, and proliferation, and promoting carcinogenesis or tumor suppression. For example, Fra2 has been reported to promote metastasis in breast cancer (Arnold et al., 2022), and to prevent it in melanoma (G. L. Chen et al., 2021). (Rampioni Vinciguerra et al., 2023)

Regarding Fra2's specific role in NSCLC, different evidence has been found. Experiments involving lung primary carcinogens, such as asbestos and tobacco smoke, showed that Fos members c-Fos and Fra1 were substantially augmented after exposure

as a consequence of increased JNK signaling, whereas Fra2 members remained constant. (Q. Zhang et al., 2005) These findings would suggest Fra2 has no significant role un lung carcinogenesis. By contrast, our laboratory has observed that Fra2 is substantially over-expressed in patient tumor tissue with respect to healthy tissue *(Figure 5D)*, and patients with higher *FOSL2* mRNA expression present significantly reduced overall survival *(Figure 5C)* *(unpublished results)*. It has also been seen that Fra2 is involved in drug resistance to EGFR tyrosine kinase inhibitor gefitinib and that it promotes the expression of GLIPR1, a mediator of cisplatin resistance. (Rampioni Vinciguerra et al., 2023)

Transdifferenciation of epithelial cells into mesenchymal cells; epithelial-mesenchymal transition or EMT; is a process integral in development and wound healing. It's also an integral process contributing to cancer progression. Different pathways control the EMT switch, responding to extracellular inductors, among which the tumor growth factor β (TGF-β) family plays a key role. (Lamouille et al., 2014) It has been shown that Fra2 expression is regulated by TGF-β1 and is required for TGF-β-induced migration of A549 NSCLC cells. Fra2 interacts with downstream TGF-β signaler Smad3, promoting its binding to P300 acetylase and its consequential acetylation. (J. Wang et al., 2014) This interaction constitutes a link between Fra2 and EMT, and thus cancer malignancy in NSCLC. Fra2 has also been linked with brain metastases in lung adenocarcinoma, constituting one of the main upstream transcriptional regulators of L1CAM, which is itself associated with distant metastases (Particularly, brain metastases) and, consequently, poor prognosis. (Feng et al., 2021)

Fra2 has been linked with the tumor microenvironment (TME) in several ways. Fra2 expression in pancreatic cancer cells activates the transcription of CCL28, leading to the recruitment of regulatory T cells and contributing to an immunosuppressive tumor microenvironment. (S. Zhang et al., 2023) On the contrary, Fra2 levels positively correlate with CD8+ T lymphocyte infiltration and tumor regression in colorectal cancer patients after chemo-radiotherapy treatment. (Xu et al., 2023) SOX2 amplification has been linked to tumor aggressiveness through a mechanism involving Fra2. Fra2, in turn, activates pro-inflammatory pathways leading to prolonged inflammation and immunosuppression, with an increase of intratumor T regulatory cells, macrophages and neutrophils, and a decrease of activated NK cells. (Njouendou et al., 2023) Tumor-associated macrophages (TAMs) is a heterogeneous denomination including tumor inhibiting macrophages (TAM1), which are activated, pro-inflammatory and anti-tumoral, and pro-tumor macrophages (TAM2), which are regulatory and anti-inflammatory. β-catenin-mediated Fra2 activation in NSCLC induces immune escape by triggering transcriptional programs associated with M2-like macrophages (CD163, CD206, IL1R1 and TGF-β). (Sarode et al., 2020) Cancer-associated fibroblasts (CAFs) contribute to ECM remodeling, angiogenesis, and tumor resistance to therapeutics. Fra2 is implicated in CAF function in breast cancer, as it regulates the transcription of Wnt5a, a secreted glycoprotein with induces angiogenesis, facilitating tumor growth. (Wan et al., 2021) In the case of ovarian cancer, Fra2 over-expression has been related to inflammasome-mediated apoptosis. (J. Li et al., 2022) Consequently, Fra2's function in the TME varies widely across tumor types, and ranges from immunosuppression and low-level persistent inflammation to the promotion of anti-tumoral immune response.

Regarding Fra2's possible role in the cell cycle, the use of inhibitors of CDK4/6 increased the expression of AP-1 members such as c-Jun, JunB, and Fra2, hinting at their possible role as mediators of resistance to this kind of therapy, as well as their implication

in the cell cycle, well documented in c-Jun and JunB, but not in the case of Fra2. (Song et al., 2023)

Much of cancer research has been focused on finding a "cure" for the disease as a whole. However, the capacity of cancer cells to adapt in a neo-Darwinian manner through epigenetic plasticity and genome instability makes this possibility unlikely. On the other hand, properly understanding the mechanisms involved in cancer progression and targeting these processes, may eventually lead to the chronification of cancer, increasing survival and quality of life of cancer patients. (Swanton et al., 2024) This perspective highlights the importance of uncovering the disease mechanisms in which Fra2 specifically, and AP-1 broadly take part, moving one step closer to the establishment of cancer as a chronic, largely asymptomatic, future disease.

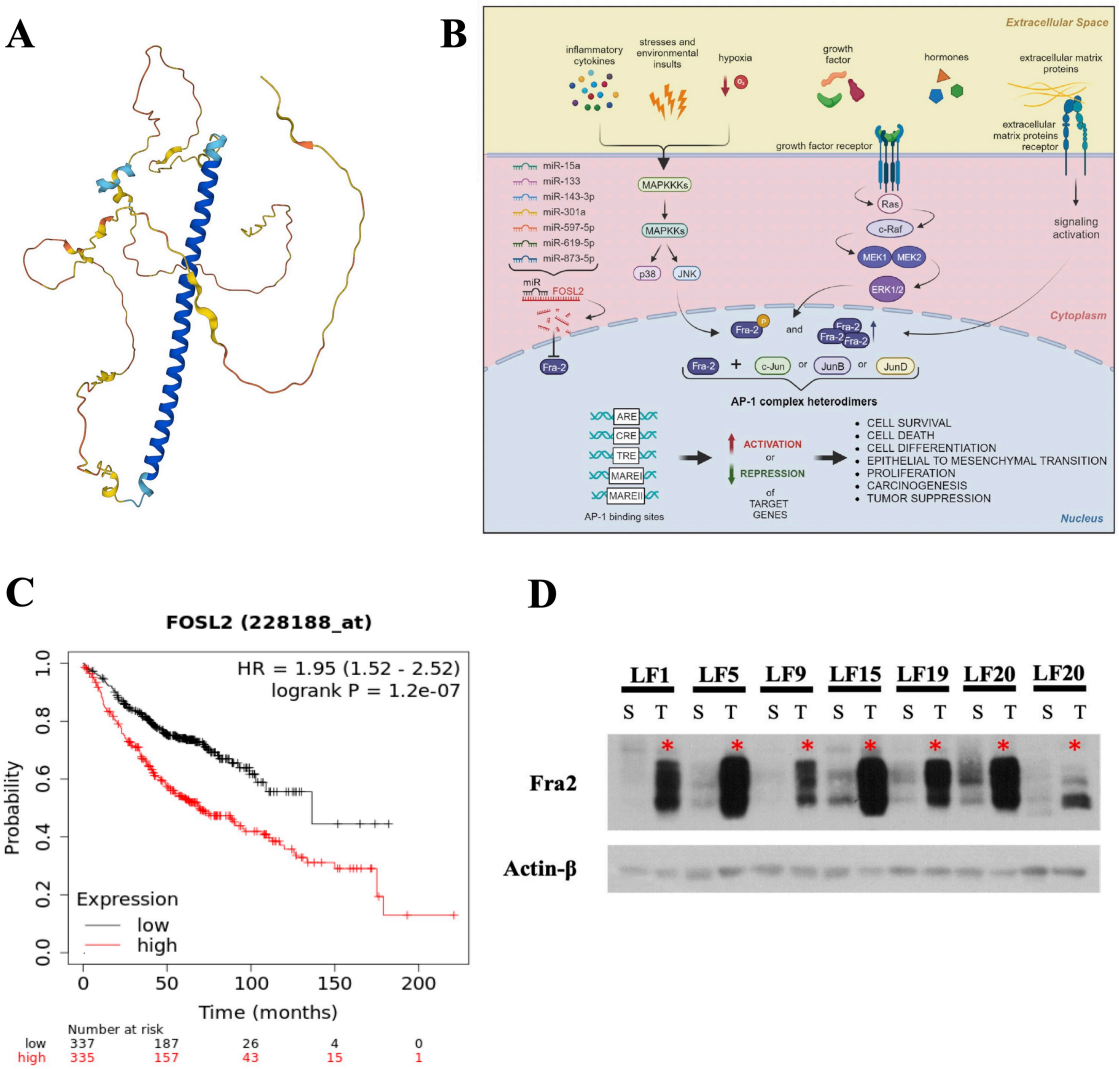

Figure 5. **Fra2, AP-1's newest member: Structure, regulation, and role in NSCLC carcinogenesis.** ***A.*** Computational prediction of Fra2's structure using AlphaFold Monomer v2.0 pipeline, as its structure has not yet been elucidated. Extracted from AlphaFold Protein Structure Database. ***B.*** Complex regulation of Fra2 in cancer. Extracted from (Rampioni Vinciguerra et al., 2023). ***C.*** Kaplan-Meyer survival curves of NSCLC patients with high and low *FOSL2* mRNA expression. ***D.*** Unpublished AP-1 expression data from tumor and healthy tissues from NSCLC patients.

Objectives

To better understand AP-1's, broadly, and Fra2's, specifically, function in the regulation of the cell cycle of cancer cells, the following objectives arise:

- Synchronize the cell cycle of a population of osteosarcoma U2OS cells using thymidine excess.

- Verify the synchronization of osteosarcoma U2OS cells by analyzing variation in whole genomic content across different times, and variation in protein abundance of representative cyclins.

- Study the variation of protein abundance of AP-1 (Jun and Fos) members across the cell cycle.

- Study the variation of mRNA abundance of AP-1 (Jun and Fos) members across the cell cycle.

- Compare patterns of AP-1 (Jun and Fos) family members across the cell cycle at the protein and mRNA level to infer the level at which their regulation in the cell cycle takes place.

- Integrate the obtained data with previous studies that cover the implication (Or possible implication) of certain AP-1 (Jun and Fos) members in the cell cycle.

Results

To analyze differences in specific markers across the cell cycle, it was firstly necessary to obtain a population of cells that homogeneously progressed across the cell cycle, so that they could be recovered at different times after release. This was performed using U2OS osteosarcoma cells, that were synchronized using excess thymidine double blockage. This specific synchronization method prevents cells from progressing across the G_1/S checkpoint *(Figure 6)*. Following cell cycle release, cells were recovered at that moment, and every 2 hours thereafter. Cells in hour 2 weren't recovered, as they present a recovery time after thymidine removal, and so progression after the cell cycle doesn't take place until afterwards.

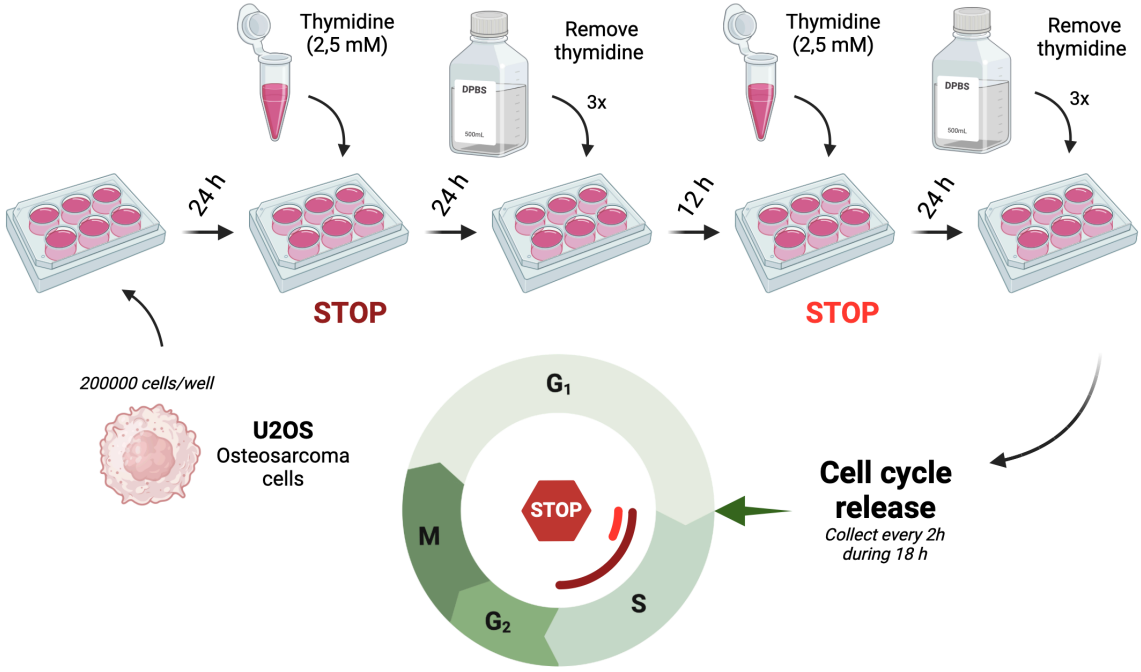

***Figure 6.* Synchronization of U2OS osteosarcoma cells using double thymidine blockage at G_1/S.** Cells were plated at 200000 cells/well in P6 plates. After 24 h of growth, thymidine 2,5 mM was added. After 24 hours of blockage in G_1/S, thymidine was removed by PBS washing. Following 12 hours of growth, thymidine 2,5 mM was added. After 24 hours of blockage in G_1/S, thymidine was removed by PBS washing, allowing cell cycle progression, and cells were collected at 0, 4, 6, 8, 10, 12, 14, 16 and 18 hours. Figure constructed using BioRender.

Variation in genomic content across the cell cycle

To verify the synchronization of the cell cycle of osteosarcoma U2OS cells, whole genomic content was analyzed across different times after cell cycle release. This was performed using propidium iodide staining, an intercalating agent that binds to nucleic acids, on ethanol-fixated whole cells. Flow cytometry analysis showed the following *(Figure 7)*.

On the one hand, analysis of exponentially grown U2OS osteosarcoma cells shows two main peaks and a plateau between them. The first peak corresponds to the population of cells in G_0/G_1, which have one full load of genomic DNA. The plateau corresponds to

the population of cells in S, as they are in the process of duplicating their DNA and so show increasing propidium iodide intensity. The second peak corresponds to the population of cells in G_2/M, as cells in those stages of the cell cycle present double the quantity of genomic DNA than those in G_0/G_1. After M phase, and so when mitosis has taken place, genomic content is halved back again.

On the other hand, synchronized cells show a main peak of cells that progress across the cell cycle starting from G_1/S. At 0 hours, a main peak can be seen at a propidium iodide intensity corresponding to the start of the S phase. At 4 hours since release, the peak that represents the synchronized population of cells has increased the propidium iodide intensity, as DNA replication is taking place during the S phase. At 6 hours, the peak progresses further, closer to the propidium iodide intensity that corresponds to G_2/M. At 8-12 hours since cell cycle release, the maximum number of cells in G_2/M is reached, and, consecutively, the peak corresponding to G_0/G_1 starts to increase until the cell population at 14 to 18 hours resembles an exponentially grown cell population.

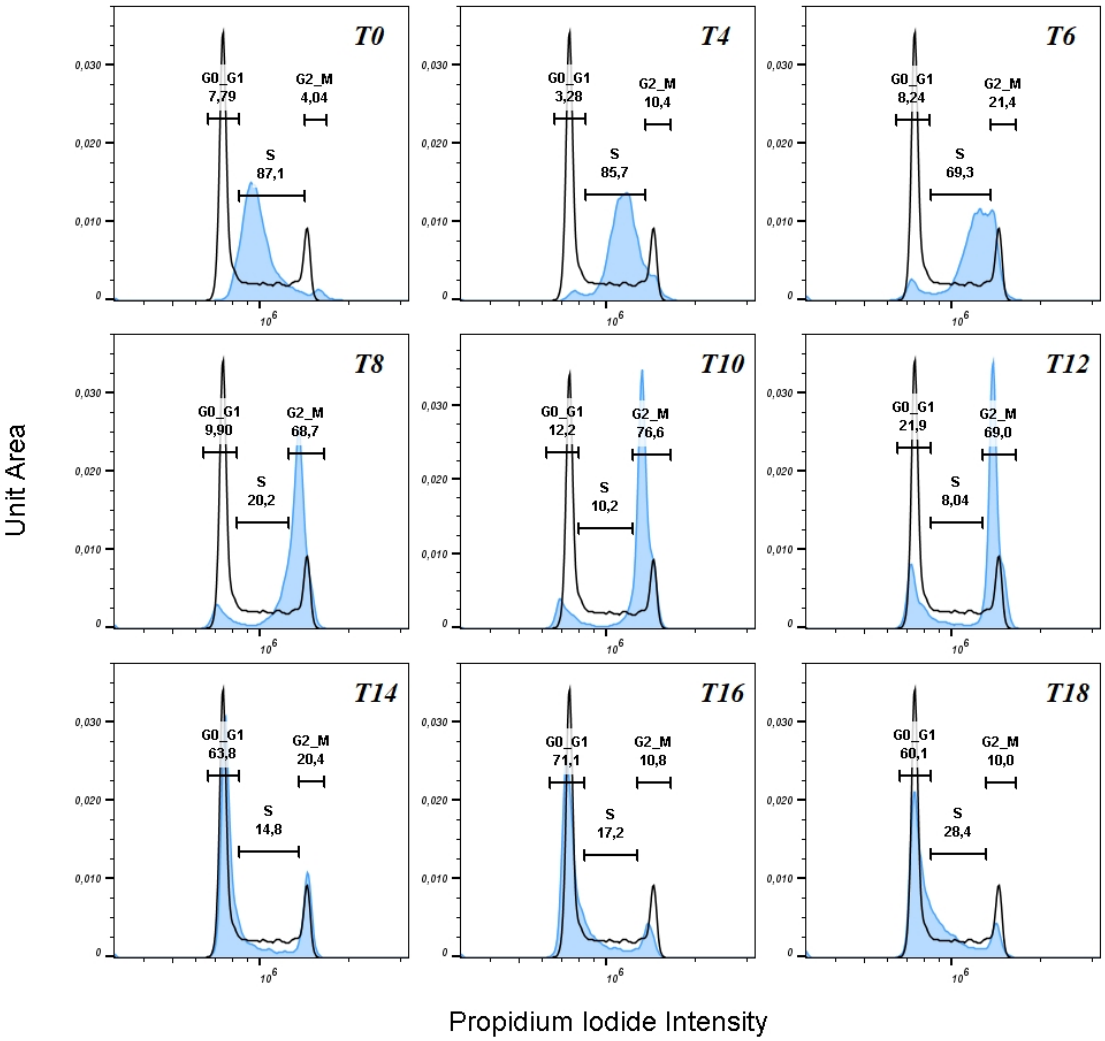

Figure 7. **Genomic content variation across the cell cycle in osteosarcoma U2OS cells.** Histograms showing total DNA (X-axis) by propidium iodide staining and cell number (Unit Area) (Y-axis) across different times (h) after cell cycle release (T0-T18), as well as in a cell population with exponential growth (Overlay). Regions corresponding to G_0/G_1, S and G_2/M phases and their relative abundance

are highlighted. N2 shown (See all in *Annex*). Data obtained using CytExpert Version 2.3 software. The flow cytometry results were analyzed using FlowJo™ v10.8 Software (BD Life Sciences).

Variation of protein abundance of AP-1 (Jun and Fos) members across the cell cycle

The variation of protein abundance of AP-1 (Jun and Fos) members across the cell cycle was assayed by performing Western Blot analysis of protein extracts obtained at different times after cell cycle release. Drastically different patterns of protein expression were perceived among AP-1 members *(Figure 8)*.

In the case of cyclin protein expression, the following was observed. Cyclin E was mostly expressed at the G_1/S transition, with a mild decline after 10 h following cell cycle release, when cells reached G_2/M. Cyclin A increased 8 hours after cell cycle release, peaking at hours 10-12 (G_2/M), and decreasing from there on. Finally, Cyclin B increased 8 hours after cell cycle release, peaking at 12 hours (M), and decreasing afterwards.

In the case of Jun family members, the following was observed. Firstly, c-Jun expression increases after G_1/S release, peaking at 12 hours, and slowly decreasing afterwards. This expression pattern shows a significant correlation with cyclin B protein expression and, to a lesser extent, cyclin A expression. Then, JunB expression drastically peaks shortly after cell cycle release, at 4 hours and the start of S phase, slowly decreasing until 12 hours. After that point, JunB greatly decreases between 12 and 14 hours, stabilizing afterwards. Lastly, JunD, considering the different experimental replicates, didn't vary significantly across the cell cycle, even though its expression seemed to be marginally higher after cell cycle release.

In the case of Fos family members, the following was observed. First, c-Fos expression drastically peaks shortly after cell cycle release, at 4 hours and the start of S phase slowly decreasing until 12 hours, as cells reach G_2/M. After that point, c-Fos greatly decreases between 12 and 14 hours, stabilizing afterwards. Even though FosB overall expression is much lower than c-Fos, it follows an almost identical pattern, with high expression at the start of the S phase and slow decrease afterwards. Fra1's expression also peaks at 4 hours after cell cycle release. However, Fra1 expression remains relatively stable from 4 hours to around 12 hours, decreasing subsequently. That is, Fra1 expression increases at the start of S phase, and remains relatively stable until G_2/M. Finally, Fra2 follows a very particular pattern, with a higher basal expression than other AP-1 members, and with a stable increase in expression from 4 to 8 hours, corresponding with most of the S phase, before returning to basal expression levels.

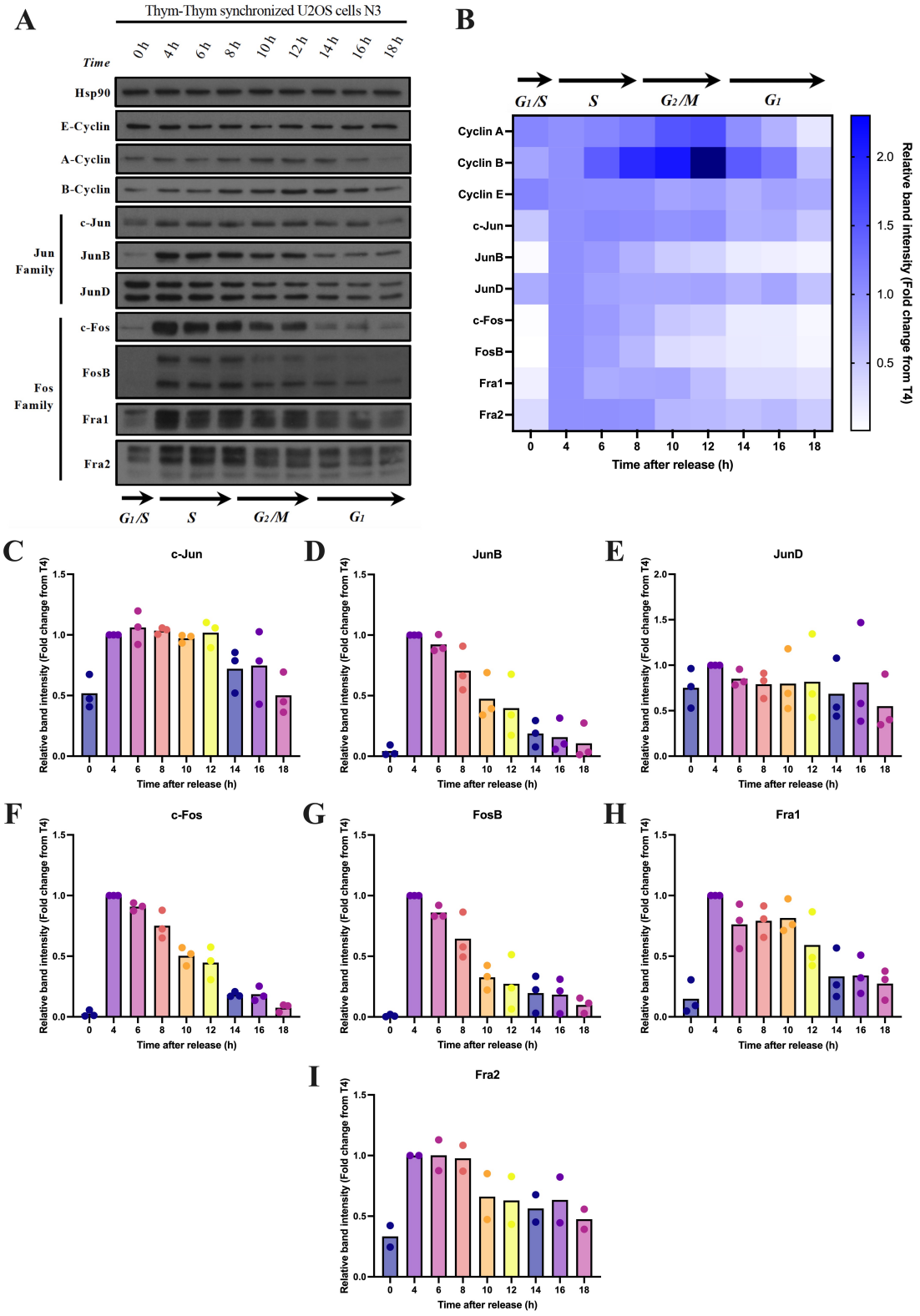

Figure 8. **AP-1 protein level variation across the cell cycle in osteosarcoma U2OS cells.** ***A.*** Western Blot showing the expression of different cyclins and AP-1 members following cell cycle release (N3 shown (See all in *Annex*)). ***B.*** Heatmap representation of protein fold change (Relative to T4) across the cell cycle. Individual bar plot representations of protein fold change (Relative to T4) of ***C.*** c-Jun ***D.*** JunB ***E.*** JunD ***F.*** c-Fos ***G.*** FosB ***H.*** Fra1 and ***I.*** Fra2. Quantified using Fiji (ImageJ). Analysis performed using GraphPad Prism 9.5.0. Ordinary one and 2-way

ANOVA with multiple comparisons between the means of every time point. Significatively relevant pairwise comparisons shown in *Annex*.

Variation of mRNA abundance of AP-1 (Jun and Fos) members across the cell cycle

The variation of mRNA abundance of AP-1 (Jun and Fos) members across the cell cycle was assayed by performing reverse transcription quantitative polymerase chain reaction (RT-qPCR) analysis of mRNA samples obtained at different times after cell cycle release. Drastically different patterns of mRNA expression were perceived among AP-1 members *(Figure 9)*.

In the case of Jun family members, the following was observed. Firstly, *JUN* expression increases after G_1/S release, topping at 10 hours, and slowly decreasing afterwards. Similarly to protein data, *JUNB* expression drastically peaks shortly after cell cycle release, at 4 hours and the start of S phase, slowly decreasing until 12 hours, and stabilizing afterwards. Lastly, again like in the case of protein expression, *JUND* didn't vary significantly across the cell cycle, with slightly higher expression at the start of the experiment.

In the case of Fos family members, the following was observed. First, *FOS* expression peaks shortly after cell cycle release, at 4 hours and the start of S phase, slowly decreasing as cells progress through the cell cycle. Nonetheless, the magnitude of this increase in expression is remarkably lower than in other AP-1 members. *FOSB*, also increases at 4 hours and the start of S phase, diminishing afterwards, however to a far greater extent than *FOS*. *FOSL1*'s mRNA expression, just as in the case of protein expression, increases shortly after release, and decreases afterwards in a much slower manner, maintaining high expression until G_2/M. Finally, *FOSL2* shows an induction only at 4 hours after cell cycle release, with relatively stable mRNA levels after that point until the conclusion of the experiment.

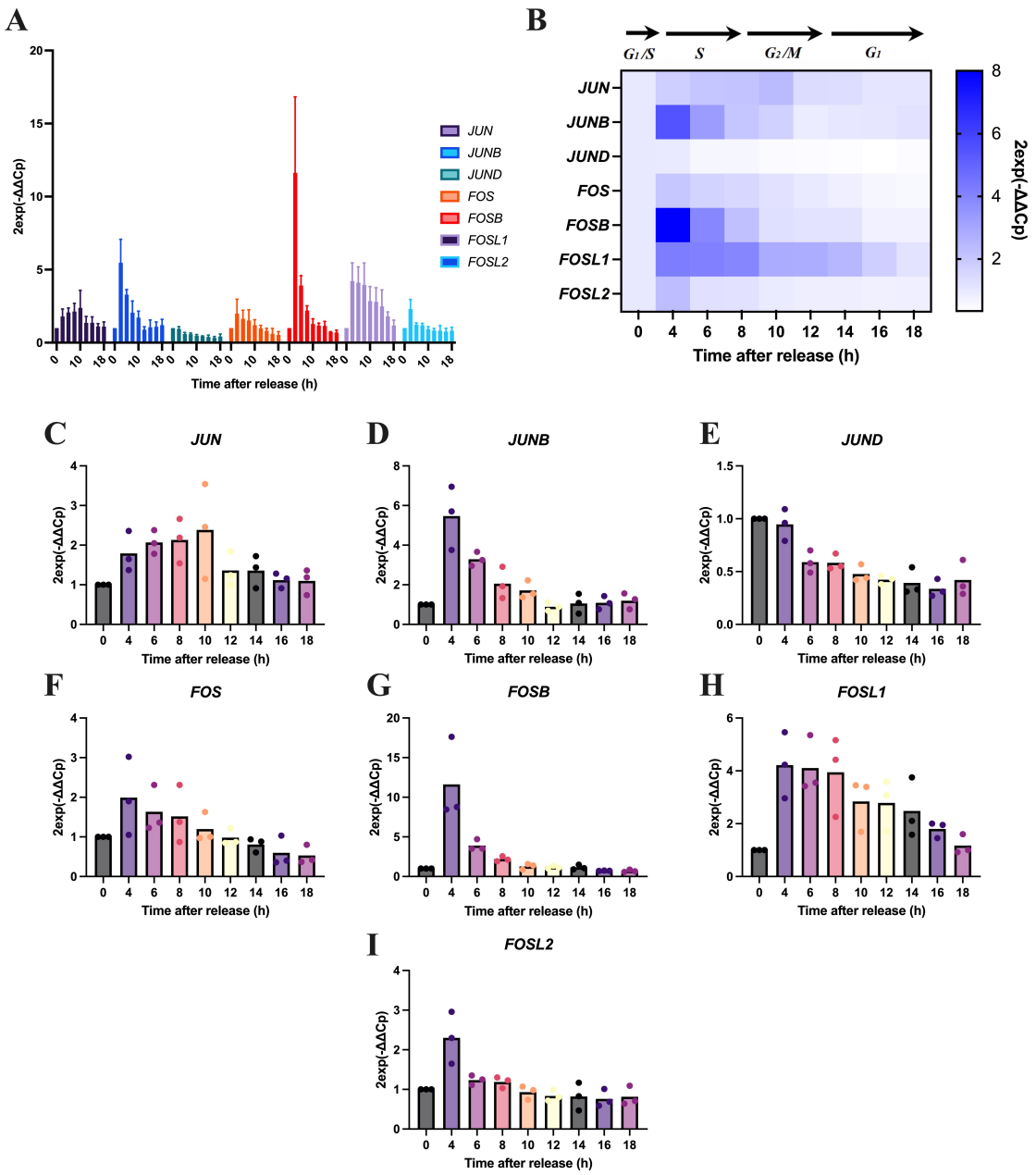

Figure 9. **AP-1 mRNA level variation across the cell cycle in osteosarcoma U2OS cells.** RT-qPCR was performed on U2OS osteosarcoma cells synchronized using double-thymidine. Data is expressed as 2exp(-ΔΔCp), where Cp is the amplification cycle of detection. Barplot (***A***) and heatmap (***B***) representation using *RPS26* as housekeeping gene for normalization. Individual bar plot representations of mRNA variation of ***C.*** *JUN* ***D.*** *JUNB* ***E.*** *JUND* ***F.*** *FOS* ***G.*** *FOSB* ***H.*** *FOSL1* and ***I.*** *FOSL2* using *RPS26* as housekeeping gene for normalization. Analysis was performed using GraphPad Prism 9.5.0. Ordinary one and 2-way ANOVA with multiple comparisons between the means of every time point. Significatively relevant pairwise comparisons shown in *Annex*. Three experimental replicates were performed.

Discussion

In the present study, U2OS-UTA6 osteosarcoma cells (Englert et al., 1995) were used to study the variation of AP-1 (Jun and Fos) members across the cell cycle, even though the focus of the lab group is on non-small cell lung carcinoma (NSCLC), as protocols for cell cycle synchronization in NSCLC cell lines (Like NCI-H23, NCI-H1395, NCI-H2030 etc.) are not as established as in the case of other cell lines, such as HeLa or U2OS cells. In fact, thymidine and other synchronization methods have been widely used to study the cell cycle in U2OS cells. (da Costa-Nunes et al., 2023) (Medema et al., 1998) (Pérez-Benavente et al., 2022) U2OS are also easy to work with and present a relatively fast doubling time (< 24 hours), which is a requirement for double thymidine synchronization. Finally, U2OS synchronization results are meant to serve as an initial model and general approximation to infer AP-1's behavior across the cell cycle in cancer cells, which will be studied more specifically in the future, as well as serve as a base for the study of Fra2's specific function, particularly in the cell cycle, in NSCLC.

Analysis of whole genomic content and protein expression of representative cyclins allowed the verification of the double thymidine synchronization in U2OS osteosarcoma cells. From these results, different timeframes can be defined, corresponding to the distinctive phases of the cell cycle. The start of the experiment, that is, 0 hours, corresponds to G_1/S or the start of the S phase, showing highest expression of cyclin E. The S phase proper would correspond to the period between hours 0-4 and 8 of the experiment. In this period, cells show intermediate DNA amounts to those of one and two whole genomic copies. G_2/M would correspond to the period between 8 and 12 hours, which matches the period that shows the most cyclin A expression. Here, cells show double genomic content as cells in G_0/G_1. Mitosis takes place around 12 hours after release, corresponding with the peak in cyclin B. The remaining timeframe (14-18 hours) corresponds to a population of cells mostly in phase G_1 of the cell cycle, with DNA amounts corresponding to one genomic copy. The definition of these timeframes for this synchronization methods and cell line specifically, was crucial for posterior relation of expression data at the protein and mRNA level of AP-1, with specific phases of the cell cycle of cancer cells.

During synchronization, cells that didn't seem to progress across the cell cycle were observed, as well as some cell populations that didn't transverse the cell cycle at the same pace as the main population. This first population of cells remained in G_0 throughout the experiment, and so, as the synchronization method performed is based on blocking cells that transverse the restriction point at G_1/S, won't be affected by thymidine and will remain, perhaps complicating the inferring of results. As most AP-1 members seem to be induced during the cell cycle, these deviations are expected to be minimal. Regarding cells that progressed at a different pace, they may have escaped thymidine blockage at G_1/S, either because the time between the first thymidine release and the second thymidine addition exceeded 12 hours, causing some cells to have already progressed across S phase at the time of blockage, or because thymidine synchronization blocks cells that are undergoing replication, and so the population of cells is less precisely defined than with methods that induce blockage at cell cycle checkpoints. Furthermore, during thymidine synchronization, cells progressively desynchronize as they divide. (Nowak et al., 2023) To improve the synchronization of osteosarcoma U2OS cells, it may be advisable to use a more precise synchronization method in the future, such as thymidine-

nocodazole synchronization, which would allow cells to progress from G_1/S after thymidine release, with nocodazole blocking them again in G_2/M, so that expression patterns of AP-1 members during G_1/S to G_2/M would be clearer. (He et al., 2017) This would allow clearer definition of timeframes corresponding to different phases, narrower peaks and easier to infer differences in expression between AP-1 members across the cell cycle.

For the evaluation of protein abundance changes, Western Blotting was performed. Western Blotting is an antibody-based experimental technique used to quantify target proteins in a complex mixture extracted from cells or tissues. Even though alternative techniques have appeared, WB is still for many the technique of choice for protein detection, mainly as enzyme-linked immunosorbent assay (ELISA) lacks loading controls, immunofluorescence is an *in-situ* technique, and mass spectrometry (MS) presents a high cost. (Tie et al., 2020) It is important to remember still, WB constitutes a semi-quantitative technique, which presents significant reproducibility issues. (Singh et al., 2021) Therefore, to verify and expand the present results, MS-proteomics will be performed to further analyze changes in protein abundance of AP-1 across the cell cycle, as well as to study variations in phosphorylation sites of AP-1, especially in the case of Fra2. During WB analysis, several of the already stated problems arose. Firstly, during quantification, data ought to be represented as an intensity ratio between a control sample, and the present sample. The best way to express the present data would have been as the ratio of normalized intensity from the different times, and normalized intensity at the start of the experiment (RT-qPCR data are expressed this way). In certain cases, expression of AP-1 members at the start of the experiment was negligible, and so to reduce dispersion in data between experimental replicates, data were expressed as a ratio between normalized intensities of different samples, and those at 4 hours since cell cycle release. Secondly, reproducibility problems occurred, especially in the case of Fra2 and Cyclin E. Regarding Fra2, data obtained in the first experimental replicate significantly varied with those obtained from the remaining experimental replicates, even though the other AP-1 members showed almost identical expression patterns. Consequently, expression data of Fra2 from the first experimental replicate was excluded from the analysis, and a subsequent experimental replicate should be performed to verify the results. In the case of cyclin E, variation of this protein across the cell cycle slightly varied across replicates, even though its expression differences were already expected to be lesser to those of cyclin A and B. Still, a similar pattern to the expected one was observed.

For the evaluation of mRNA abundance changes, RT-qPCR was performed. Fluorescence-based reverse transcription, real-time quantitative PCR (RT-qPCR) is a highly sensitive method for quantification of specific RNAs, and has become a common tool in basic research, functional genomics, biotechnology, and medicinal, forensic, and water quality diagnostics. (Botes et al., 2012) It was chosen over other techniques, as it is faster and more sensitive than Northern Blotting or microarrays, and cheaper and less analysis intensive than RNA-seq or digital PCR (dPCR), especially considering the panel of genes to be analyzed was only 9 different genes, an appropriate amount for RT-qPCR analysis. (Smith & Osborn, 2009) RT-qPCR detection of the different 9 genes chosen for analysis was successful across three experimental replicates. However, it must be stated that a significant dispersion was observed in data obtained from different replicates, especially regarding the expression peaks of genes like *JUN*, *JUNB*, *FOSB* and *FOSL1*. Different housekeeping genes were chosen for normalization based on prior lab experience. These were *GUSB* and *RPS26*. *GUSB* encodes β-glucuronidase, a hydrolase

that degrades glycosaminoglycans, including heparan sulfate, dermatan sulfate, and chondroitin-4,6-sulfate. (Khan et al., 2016) It has been proven as one of the best normalization genes for RT-qPCR experiments in different types of cancer cells, including osteosarcoma U2OS cells. (Razavi et al., 2019) (Dong et al., 2022) *RPS26* encodes ribosomal protein S26 which, on the other hand, is one of the approximately 80 proteins that form the eukaryotic ribosome. It has been widely used as an invariant control for gene regulation experiments in eukaryotic cells and tissues. (Vincent et al., 1993) (Bai et al., 2020) When comparing results obtained after normalization with both genes, those that used *GUSB* show lesser reproducibility and larger dispersion than those obtained with *RPS26 (See Annex)*. For this reason, *RPS26* was chosen as the main housekeeping gene for normalization in RT-qPCR.

As it was already stated, AP-1 is involved in a myriad of cellular processes, taking part in the onset and development of different pathologies, and with a particular implication in cancer. One of the main ways AP-1 contributes to cancer progression is through the control of cell proliferation and cell cycle progression. The present study aids the characterization of concurrent / simultaneous AP-1 subfamilies Jun and Fos across the cell cycle and contributes to characterizing their role in cancer proliferation and progression.

Jun Family

As is the case for most AP-1 members, c-Jun's role in cancer, and specifically in proliferation and cell cycle control in cancer, is complex. The main described role for c-Jun in cell cycle control is as an inducer of cyclin D1. Phosphorylation of c-Jun in its N-terminal domain by the p34(cdc2)-cyclin B kinase during mitosis and early G_1 increases its transactivation potential, leading to cyclin D1 expression and G_1 progression through Rb phosphorylation by CDK4/6 and Cyclin D complexes. (Bakiri et al., 2000) The observed expression pattern of c-Jun (at the protein and mRNA levels), with a steady increase across the S and G_2 phases, and a slow decline after the M phase with cells progressing across G_1, would correlate with its phosphorylation in G_2/M, leading to induction of cyclin D1 and its posterior degradation. On the other hand, c-Jun has also been shown to antagonize the activity of cell cycle repressor p53, which causes cells to undergo apoptosis if excessive DNA damage is present, repressing cyclin D and E among others. (Eferl et al., 2003) This way, c-Jun contributes to cancer development and the control of the cell cycle not only with the induction of cyclin D1 and the progression through G_1, but also preventing apoptosis and cell cycle blockage by p53.

JunB has been generally described as a cell proliferation inhibitor, a senescence inducer and a tumor suppressor. In this sense, contrary to c-Jun, JunB phosphorylation by the p34(cdc2)-cyclin B kinase is associated with lower JunB protein levels in mitotic and early G_1 cells, favoring cell cycle progression, as JunB acts as a repressor on the cyclin D1 promoter. (Bakiri et al., 2000) This proliferator inhibitor function is also linked with JunB's inductor function on the $p16^{INK4\alpha}$ cyclin-dependent kinase inhibitor. (Passegué & Wagner, 2000) Contrarily, a cell-division-promoting activity has also been described for JunB. Cyclin A is a direct transcriptional target of JunB, and, consequently, JunB expression promotes the progression through the G_1/S checkpoint. (Andrecht et al., 2002) Furthermore, JunB's proteasome-dependent degradation in late G_2 has been proven to be necessary for the reduction of cyclin A2 levels in prometaphase, crucial for the undergoing of proper mitosis. (Farràs et al., 2008) Additionally, JunB acts as an inducer of cyclin E1 and a repressor of TGF-β2, aiding cell proliferation and tumor invasiveness.

(Pérez-Benavente et al., 2022) The observed expression pattern, with higher JunB expression (at the protein and mRNA levels) at G_1/S, with a slow decrease across S and G_2 phases and fast degradation during mitosis, coincides with its important function as a cyclin A inducer (strong induction at the start of the S phase) and as a key signaler for its degradation in prometaphase. It would correlate to a lesser extent with its function as a cyclin E inducer, but a different synchronization method may be necessary to explore its function in mid and late G_1.

Less is known about the latter Jun family member's implication in the cell cycle. However, JunD knockdown has been reported to produce cell cycle arrest at G_1 in prostate cancer cells, with reduced expression of cell cycle inducers, such as cyclin D, Ki67 and c-Myc. (Elliott et al., 2019) Furthermore, JunD binding to DNA was promoted using LHRH antagonist triptorelin in ovarian cancer, resulting in reduced proliferation and DNA synthesis, and stalling in G_0/G_1. (Günthert et al., 2002) The observed expression pattern in the case of JunD (At the protein and mRNA level), minimally varied during the assay time, with lightly higher expression at the start and end of the experiment, but taking experimental replicates into account, differences were marginal. Taking the present results and previous studies into account, JunD appears to not exert a role during the cell cycle itself (That is G_1, S, G_2 and M phases), but perhaps at the transition between G_0 and G_1, as it over and under-expression cause G_0/G_1 stalling, and its knockdown reduces cell cycle inducers, including Ki67, key in the G_0/G_1 transition. (Manoir et al., 1991)

Fos Family

The c-Fos oncoprotein has been widely studied and, consequently, what is known about its implication in the cell cycle suggests a complex landscape. On the one hand, c-Fos has been described as a cell cycle promoter, its expression being necessary through all phases of the continuous cell cycle. (Pai & Bird, 1994) In this sense, c-Fos has been described as an inducer of cyclins A, D and E, and CDKs 2, 4 and 6. (Sunters et al., 2004) (Sunters et al., 1998) (Brown et al., 1998) It has also been identified as a repressor of the cell cycle inhibitor $p21^{Cip1/WAF1}$. (Crowe et al., 2000) c-Fos mRNA levels have been described to peak at early G_1, and it has been described to exert a role in the initiation of the S phase. (Curtis Bird et al., 1990) (Vriz et al., 1992) Finally, c-Fos has been described to promote CKS1 expression and progression at G_2/M. (Oh et al., 2023) On the other hand, it's been seen that prolonged c-Fos overexpression suppresses cell cycle entry, and the proposition has arisen that c-Fos isn't essential for cell cycle progression at all. (Okada et al., 1999) (Brüsselbach et al., 1995) The observed expression pattern for c-Fos (At the protein and mRNA level), with higher expression at G_1/S and slow decrease afterwards, would correlate with its described function as an inducer, specifically of cyclins E and A, CDK2 and a repressor of $p21^{Cip1/WAF1}$. Interestingly, c-Fos exhibited the same protein expression pattern as JunB, and they both present common functions as activators of cyclins A and E, suggesting their function in the cell cycle control of cancer cells is mainly mediated as JunB:c-Fos heterodimers. The differences in mRNA and protein expression peaks for c-Fos, as protein induction is much more drastic than mRNA induction, hints at intermediate regulation levels. This may coincide with the fact that c-Fos mRNA expression has been generally described to peak at early G_1, even if most of c-Fos activity in cell cycle control takes place at G_1/S.

In contrast to c-Fos, very little has been studied regarding FosB's role in cell cycle control. Just as the case of c-Fos, FosB has been described as a direct or indirect activator of cyclin D1 expression. (Brown et al., 1998) It was also seen that FosB overexpression

didn't have a significant negative effect on cell proliferation, which would indicate that FosB is not a negative regulator of growth. (Dobrzanski et al., 1991) The observed expression pattern for FosB (At the protein and mRNA level), with higher expression at G_1/S and slow decrease afterwards, significatively correlates with that observed for JunB and c-Fos, even though noteworthy background information is lacking to back this claim. Still, the initial hypothesis would be that not only JunB:c-Fos heterodimers are responsible for promoting the progression across G_1/S, but that JunB:FosB heterodimers, to a lesser extent (As its expression in cancer cells is much lower) contribute to this function.

Fra1's overall pathological function isn't wholly understood, much less its specific function in the regulation of the cell cycle of cancer cells. However, it is known that Fra1 plays a role promoting the G_1 transition, as the ERK1/2-Fra1 axis is responsible for the over-expression of cyclin D1 that contributes to NSCLC progression. (Al-khayyat et al., 2023) (Gao et al., 2020) Inversely, Fra1 has been proven to be essential for AKT's activation and induction of cyclin B1, necessary for G_2/M progression. (X. Zhang et al., 2016) Fra1 knockdown has been shown to cause proliferative block and apoptosis, and cyclin A has been revealed as one of its main targets. Another described target of Fra1 is JunB, which further interacts with the cyclin A promoter and favors its expression. (Casalino et al., 2007) The observed expression pattern for Fra1 (at the protein and mRNA level), with higher expression across the S phase that is maintained after G_2/M before diminishing, significatively correlates with Fra1's described function as an inducer of JunB, cyclin A, and cyclin B, which would explain why its expression is maintained across our cell synchronization assay much more than JunB, c-Fos or FosB, as their degradation may be necessary for M progression. Fra1's maintained expression across G_2/M may also be related to its described function as an upstream regulator of cyclin D, just as c-Jun, even though a different synchronization method may be necessary to properly detect changes in G_1. With the different patterns observed for AP-1 members, and taking into account Fos members can only act as heterodimers with Jun, Fra1 may act as a JunB:Fra1 heterodimer during G_1/S and early S phase, and as a c-Jun:Fra1 heterodimer at G_2/M.

Fra2 is the newest member of AP-1, and so its function is one of the least studied and understood of them all. Regarding its role in the regulation of the cell cycle, very little is known. It's been found, however, in glioblastoma, that Fra2 silencing leads to significant diminishing in cell cycle drivers' expression, such as cyclins D1 and E1. (Luo et al., 2018) Furthermore, Fra2 takes part in lncRNA ITGB2-AS1-mediated cisplatin resistance by driving the inhibition of cell cycle inhibitor and apoptosis promoter, p53. (H. Chen et al., 2023) The observed expression pattern for Fra2 at the protein level presents relatively high expression levels through the cell cycle, with a marked plateau across the S phase. On the other hand, the observed expression pattern for Fra2 at the mRNA level presents similar expression levels through the cell cycle, only increasing at the start of the S phase. The present data seemingly contradict previously available studies, and even though it seems clear Fra2 takes part in promoting cell proliferation, what is known about its role in the cell cycle is mostly tangential information. Taking this study's information into account, Fra2 appears to play a role during the S-phase, coinciding with unpublished Fra2 over-expression data from the lab. Furthermore, differences at the RNA and protein level suggest that Fra2 is initially expressed at the start of the S phase but is then mainly regulated at the protein stability level, possibly through post-translational modifications, such as phosphorylation, sumoylation, ubiquitination, etc. Consequently, an interesting research line arises for the

characterization of Fra2's post-translational modifications pattern during the cell cycle, which is intended to be assayed using MS-proteomics. Finally, most about Fra2's role in cancer, and particularly in cell cycle control remains an enigma, but the present study serves as a basis for future developments.

The present study, as well as previously available information, show that AP-1 expression levels are regulated during the cell cycle and highlight the highly complex function of AP-1 in the control of the cell cycle of cancer cells. They remark that AP-1 doesn't exert its function as a monolithic and one-dimensional actor, but as a dynamic group of protein members that highly vary their relative abundance and dimerization patterns across the cell cycle in U2OS cells *(Figure 10)*. In this context, c-Jun presents itself as an important inducer across the G_1 phase, together with Fra1. JunD may act at the G_0/G_1 transition, and not during the cell cycle itself. JunB, together with c-Fos, FosB, and Fra1 appear to play a role in the progression across G_1/S. Fra1, additionally, emerges as an important factor in the progression across G_2/M, together with JunB's degradation. Finally, Fra2 may play a role in the progression past the S phase. Many questions about AP-1 remain without answer, but its implications in a myriad of devastating pathologies, and specially cancer, remark the need for its continuous study in the fight against them.

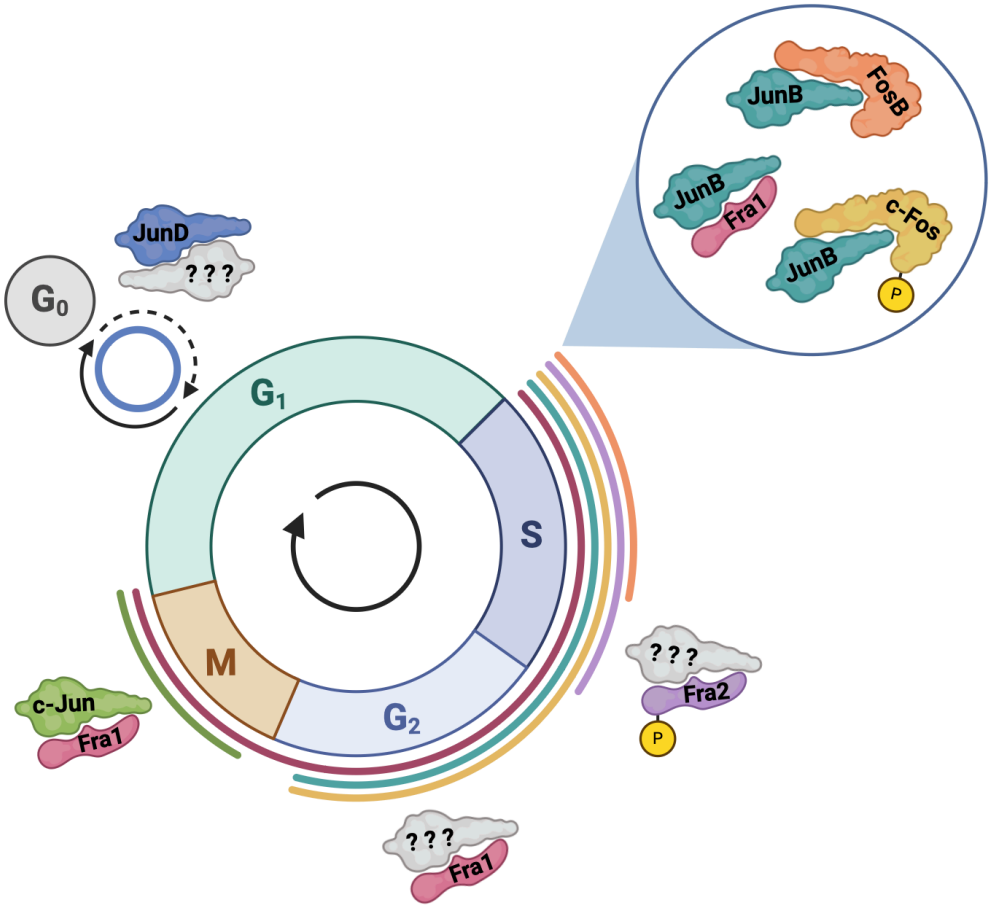

Figure 10. **AP-1 and the cell cycle of cancer cells. General conclusions.** Proposed model of AP-1 (Jun and Fos) members and their possible dimerization patterns across the cell cycle taking previous data, as well as the present expression data (at the protein and mRNA level) into account. Expression peaks highlighted for c-Jun (Green), JunB (Blue Green), JunD (Blue), c-Fos (Yellow), FosB (Orange), Fra1 (Magenta) and Fra2. (Purple). Proposed intermediate levels of regulation marked (P). Constructed using BioRender.

Parallel studies

In parallel to the study of AP-1's variation across the cell cycle, the specific function of Fra2 in NSCLC has been under study in the lab. This is because, contrarily to other cancer types, Fra2 overexpression correlates with poor survival.

To uncover its function, Fra2 is being silenced, using different silencing RNAs (siRNAs), as well as over-expressed, using different constructions, in different NSCLC cell lines (NCI-H1395, NCI-H2030, NCI-H23), as well as in osteosarcoma U2OS cells. Over-expression constructions with GFP and FLAG tags have been built to more easily report the recombinant protein. In the latter case, the construction presents a reporter GFP after an internal ribosomal entry site (IRES), leading to equal productions of Fra2 and GFP, and is used in U2OS-UTA6 cells, taking advantage of the TetOff system, that induces Fra2 over-expression in the absence of tetracycline from the culture media. Different assays are being performed on the resulting cells, including Western Blot of relevant markers, cell cycle, migration and invasion assays, transcriptomics, ChIP-seq, MS-proteomics and phosphoproteomics. This will allow to better understand Fra2's targets, its function and regulation.

After cell culture studies, it is expected to move on to the creation of mouse xenograft models using stable Fra2 over-expressing or silenced cells to study possible effects on tumor growth and metastatic potential on preclinical models.

These studies will allow the obtaining of a holistic understanding of Fra2's function in NSCLC, and cancer more broadly.

Further studies

The discovery of the different expression patterns of AP-1 members across the cell cycle highlights the need for further studies in this direction:

- To improve the characterization of AP-1 expression patterns across the cell cycle, it would be ideal to perform more informative synchronization methods, as would be the case of double thymidine-nocodazole synchronization, as well as to define synchronization protocols that could be performed on NSCLC cell lines, towards better extrapolating the results to the realities of the pathology.

- To better understand the regulation of AP-1 across the cell cycle, the post-translational modifications of these proteins across the cell cycle should be put under study. It would be specially interesting to study Fra2's uncharacterized phosphorylation pattern across the cell cycle using MS-based phosphoproteomics.

- The study of the function of different AP-1 members in the cell cycle, and specifically Fra2, will be improved by the understanding of their immediate and downstream targets, as well as their mechanisms of regulation through upstream signaling.

- Due to the highly dynamic and complex action of AP-1 through different dimerization patterns, studying how these patterns change across the cell cycle through co-immunoprecipitation (CoIP) would travel a long way into understanding the particularities of AP-1 in the cellular process.

- Finally, identifying the pathways that activate AP-1 and its effectors in cancer cells opens the discovery of new biomarkers and the possibility of studies of early therapeutic intervention in patients.

Conclusions

Considering the different results obtained during the development of the present study, the following conclusions can be drawn:

- A synchronized population of U2OS osteosarcoma cells that homogeneously progressed across the cell cycle was obtained, thus allowing the analysis of AP-1 at different levels during this cellular process. This was verified by the analysis of variation in total genomic content and different representative cyclins. However, certain cells were able to evade synchronization.

- The variation in total genomic content and expression of different cyclins in U2OS allowed the definition of approximate timeframes corresponding to cell cycle phases; G_1/S (0 hours), S (0/4-8 hours), G_2/M (8-12 hours), M (12 hours) and G_1 (14-18 hours).

- Drastically diverse patterns of mRNA and protein expression were observed with the different AP-1 members, with further disparities at the mRNA and protein levels that hint at intermediate regulation levels in the case of c-Fos and Fra2.

- Integration of the obtained data with available data allowed the construction of a hypothetical model for AP-1's involvement in the cell cycle, in which c-Jun presents itself as an important inducer across the G_1 phase, together with Fra1. JunD may act at the G_0/G_1 transition. JunB, together with c-Fos, FosB, and Fra1 appear to play a role in the progression across G_1/S. Fra1, additionally, emerges as an important factor in the progression across G_2/M, together with JunB's degradation. Finally, Fra2 may play a role in the progression past the S phase.

- Taken altogether, the present study is an all-inclusive first approximation to AP-1 in the cell cycle of cancer cells, serving as an important backbone for future more specific studies focused on some of the lesser studied members of AP-1, as well as those focused on particularities regarding their regulation and dimerization patterns.

Materials & Methods

Cell culture

Cell culture was performed using osteosarcoma U2OS-UTA6 (RRID:CVCL_XF79) cells grown with High-Glucose Dulbecco Modified Eagle's Medium (DMEM) (Sigma-Aldrich) + 10 % fetal bovine serum (FBS) + 1 % penicillin / streptomycin (P/S). These cells were provided by the American Type Culture Collection (ATCC), presenting driver mutations in *PPM1D* (p.Arg458Ter; c.1372C>T).

Thymidine synchronization

Synchronization of the cell cycle in cells in culture allows to check for changes in specific markers along the cell cycle. The protocol used is based on thymidine excess and is considered a soft synchronization method. Thymidine excess blocks ribonucleotide reductase, leading to deoxyribonucleotide depletion and stopping replication, causing the halting of cells in the G_1/S checkpoint. This synchronization is performed using osteosarcoma U2OS cells, as they work well with this specific protocol. Cells are seeded in day 1 at 200000 cells per well in P6 plates. After 24 hours, in day 2, thymidine 2,5 mM is added to the culture medium. Once another 24 hours have passed, in day 3, thymidine is removed, and cells are washed thrice with PBS before adding culture media. 12 hours later, thymidine 2,5 mM is added once again to the culture media in day 4. In day 5, 24 hours later, thymidine is removed, and cells are washed thrice with PBS. Culture media is added, and so cells are allowed to progress along the cell cycle. Cells are then recovered at different times: 0, 4, 6, 8, 10, 12, 14, 16 and 18 hours. This way, cells are allowed to fully progress across the cell cycle.

Flow Cytometry

Cytomic analysis of DNA content in cell monoculture

To analyze the DNA content of cells in monoculture, the cell media is transferred into a 15 mL centrifuge tube. Cells are washed with PBS (37ºC), which is afterwards collected in the centrifuge tube. Cells are incubated with trypsin for 5 minutes at 37ºC. Consecutively, cells are resuspended in culture media and collected in the centrifuge tube. Cells are centrifuged at 400 g for 5 minutes. The supernatant is removed, and the pellet is resuspended in 100 µL of PBS (37ºC). Cells are fixed by slowly adding 1 mL of ethanol 70 % while gently vortexing. Cells can be preserved at -20 ºC until further use. Cells are stained by centrifuging 400 g for 5 minutes at 4ºC and resuspending in staining solution (Propidium iodide 5 µg/mL and RNAse 100 µg/mL in PBS). Incubation takes place during 16-18 h at 4ºC and darkness. Cells are then analyzed using CytoFLEX S (Beckman-Coulter). Data processed using CytExpert Version 2.3. The flow cytometry results were analyzed using FlowJo™ v10.8 Software (BD Life Sciences).

Western Blot

Cell plating and protein extraction

Cell plating concentration in P6 plates will vary depending on the specific assay and the cell lines used, but the most adequate concentration for most of the experiments performed was 150000 cells per well. The protein extraction protocol must take place on ice to avoid protein degradation during extraction. The culture medium is removed using vacuum, and wells are consecutively washed twice using 2,5 mL of cold PBS. After removing it, cells are collected using scrappers in 300 µL of lysis buffer (2 % SDS + NaCl 150 mM + Tris 67 mM + Sucrose 175 µM + 1 % Triton X100 + cOmplete protease inhibitor cocktail (Roche)) and boiled 10 minutes at 95ºC, with thorough vortex every 5 minutes. The samples are then stored at -20ºC until further use.

Protein quantification using BCA

Protein concentration is determined using Thermo Scientific Pierce BCA Protein Assay Kit. The calibration curve is prepared following the indications specified in the kit. A dilution of 1:5 is usually required for the values of the protein samples to properly fit in the linear region of the calibration curve. 10 µL of every diluted protein sample and of the calibration curve are added into P96 plates, performing two duplicates. BCA reactive A and B are then mixed in a 50 to 1 proportion and 200 µL of the mix are added to each well in the plate. The plate is then incubated during 30 minutes at 37ºC, in darkness and with 60 rpm agitation before measuring absorbance at 562 nm in Perkin Elmer Wallac 1420 Victor2 Microplate Reader spectrophotometer. Protein concentration values for the samples are then obtained by interpolation in the calibration curve.

SDS-PAGE

To separate proteins according to electrophoretic mobility, SDS polyacrylamide gel electrophoresis is performed (BioRad Mini-PROTEAN® Tetra Handcast Systems). Gels are polymerized using 1,5 mm glass plates and concentrations of acrylamide:bisacrylamide 29:1 ranging from 8 to 15 % depending on the molecular weight of the protein of interest. Stacking and resolving gels *(Table 1)* are polymerized to concentrate proteins in the samples and improve resolution. Once polymerized, gels are mounted in the electrophoresis tray and running buffer (Glycine 190 mM + Tris 25 mM + 0,1 % SDS) is added before sample loading. Samples are prepared by diluting protein extracts (As well as PageRuler Prestained Protein Ladder, 10 to 180 kDa, from ThermoFisher Scientific) in water to load 15 µg and mixed with Laemmly buffer 5x (10 % SDS + DTT 0,5 mM + Tris 250 mM + Sucrose 0,88 mM + Bromophenol Blue 3 µM). Samples are boiled during 5 minutes at 95ºC before loading. Gels are run at a constant amperage of 15 mA per gel until the electrophoresis front reaches the end of the glass plates.

Table 1. **Composition of SDS-PAGE gels at different AA:BAA percentages.** Different components are added to the solution in the specified order.

	Resolving Gel (mL)				
	8%	***10%***	***12%***	***12.5%***	***15%***
H_2O Type II	7.94	7.19	6.44	6.25	5.31
Tris pH 8.8 1,5 M	3.75	3.75	3.75	3.75	3.75
AA/BAA 40 %	3	3.75	4.5	4.69	5.63
SDS 10 %	0.15	0.15	0.15	0.15	0.15

APS 10 %	0.15	0.15	0.15	0.15	0.15
TEMED	0.015	0.015	0.015	0.015	0.015

Stacking Gel (mL)	
H_2O Type II	3.74
Tris pH 6.8 0.5 M	1.5
AA/BAA 40 %	0.75
SDS 10 %	0.06
APS 10 %	0.06
TEMED	0.006

Membrane Transfer

Proteins separated by SDS-PAGE are then transferred to a PVDF membrane by electroblotting (BioRad Mini Trans-Blot®). PVDF membranes are extremely hydrophobic and must be activated using methanol for 5 minutes, before washing twice with type II water for 2 minutes and leaving them in transfer buffer (Tris Base 50 mM + Boric Acid 50 mM) until cassettes are mounted. Cassettes are then mounted with sponges, Whatman filter paper, the SDS-PAGE gel on the negative side, and the PVDF membrane in the positive side, so that negatively charged proteins in the gel will transfer to the membrane. Cassettes are placed in the tray with transfer buffer and the transfer then takes place at constant voltage of 12 V, for 16 hours, at room temperature and in agitation.

Ponceau Staining

After dismounting the cassettes, membranes are stained using Ponceau to check that the transfer has taken place correctly, as well as the overall protein quantities of the different samples. Membranes are submerged in Ponceau solution (Ponceau 0,1% and 1% acetic acid) for 10 minutes. Destaining is then performed using acetic acid 1% until the background of the membrane is completely white. After image capture, membranes are washed twice with TBS-T (Tris 20 mM + NaCl 150 mM + 0,05 % Tween-20) for 5 minutes.

Antibody Incubation

Membranes are blocked to avoid unspecific binding of antibodies. This is performed by incubating the membranes for 1,5 hours in blocking solution (TBS-T + 5 % Milk Powder). After quickly washing the blocking solution with TBS-T, membranes are then incubated with the corresponding primary antibodies *(Table 2)* diluted in primary antibody solution (TBS-T + 5 % BSA + 0,05 % Sodium Azide) for 16-18 hours, in agitation and 4ºC. Membranes are then washed three times using TBS-T for 10 minutes to get rid of unbound primary antibodies. Subsequently, membranes are incubated with secondary antibodies *(Table 2)* diluted in blocking solution for 2 hours at room temperature. Membranes are washed three times using TBS-T for 10 minutes to get rid of unbound secondary antibodies.

Table 2. **Primary and secondary antibodies used in Western Blotting.** The specificity, as well as the species of origin, the dilution, whether they are monoclonal or polyclonal, the reference and the supplier are included.

Specificity	*Species of origin*	*Dilution*	*Monoclonal or polyclonal*	*Reference*	*Supplier*
c-Fos	Rabbit	1:1000	Monoclonal	#2250	Cell Signaling
c-Jun	Rabbit	1:1000	Monoclonal	#9165	Cell Signaling
Cyclin A	Mouse	1:5000	Monoclonal	ZRB1590	Sigma-Aldrich
Cyclin B	Rabbit	1:5000	Polyclonal	GTX100911	GeneTex
Cyclin E	Rabbit	1:1000	Polyclonal	sc-481	Santa Cruz
FosB	Rabbit	1:1000	Monoclonal	#2251	Cell Signaling
Fra1	Rabbit	1:1000	Monoclonal	#5281	Cell Signaling
Fra2	Rabbit	1:1000	Monoclonal	#19967	Cell Signaling
Hsp90	Mouse	1:10000	Monoclonal	sc-13119	Santa Cruz
JunB	Rabbit	1:1000	Monoclonal	#3753	Cell Signaling
JunD	Rabbit	1:1000	Monoclonal	#5000	Cell Signaling
Mouse IgG (HRP-conjugated)	Rabbit	1:5000-15000	Polyclonal	A9044	Sigma-Aldrich
Rabbit IgG (HRP-conjugated)	Goat	1:5000	Polyclonal	A6154	Sigma-Aldrich

Developing

Developing of the membranes is performed using chemoluminiscence. The chemoluminiscent substrate reacts with HRP conjugated with the secondary antibody, producing light that can be captured. Membranes are incubated with different chemoluminiscent kits *(Table 3)* depending on the sensitivity required. These kits contain two solutions; hydrogen peroxide and luminol and are mixed in a proportion of 1:1. Incubation time is also dependent on the protein assayed and the expected signal but is usually around 5 minutes. There is different equipment available for developing in the lab, including automatic systems such as Uviteq Alliance Q9, Amersham Imager 600 and Amersham ImageQuant 800, as well as AFGA Curix 60, that is used with AFGA CP-BU M less sensible films, and Amersham Hyperfilm ECL more sensible films. Exposition times are determined from experience in each case and adjusted for optimum signal.

Table 3. **Chemoluminiscent kits used in Western Blotting.** Chemoluminiscent kits, their sensitivity, and the supplier.

Chemoluminiscent kit	***Sensitivity***	***Supplier***
ECL Prime Western Blotting Detection Reagent	2,4 pg	Amersham
ECL Western Blotting Reagents	10 pg	Amersham
Lumi-Light Western Blotting Substrate	10 – 50 pg	Roche
SuperSignal West Femto Maximum Sensitivity Substrate	Femtograms	ThermoFisher Scientific

Stripping

When more than one protein must be assayed from one membrane, it can be useful to perform a stripping protocol on the membrane. Stripping with guanidine hydrochloride 7 M can remove the binding of secondary antibodies to primary antibodies and is thus especially useful when sequentially incubating with antibodies obtained from different animal species. If the membrane has started to dry out during developing, it is submerged in methanol for 5 minutes, followed by washing twice with type II water for 2 minutes. The membrane is treated with guanidine hydrochloride 7 M for 15 minutes, washed twice with TBS-T for 5 minutes, and then submerged in TBS-T + 3 % SDS for 20 minutes at 40ºC. A short membrane blocking of 30 minutes is performed before the rest of the protocol.

qRT-PCR

Cell plating and RNA extraction

For RNA extraction, cell plating concentration is adjusted depending on the assay to 150000 to 200000 cells per well in a P6 plate. After growth, culture medium is removed with vacuum and wells are washed with 2,5 mL of cold PBS. Afterwards, cells are scraped in 200 µL of cold PBS and immediately frozen in dry ice. They are stored at -80ºC until further processing. RNA extraction is performed using Roche's High Pure RNA Isolation kit, obtaining 30 µL RNA samples that must be quantified with ND1000 Nanodrop spectrophotometer (Thermo Fisher Scientific).

Retrotranscription from mRNA to cDNA

To obtain cDNA samples that can undergo qRT-PCR, retrotranscription must take place using the RNA samples extracted. After quantification, 1 µg or RNA is required to undergo retrotranscription using Takara's PrimeScript Reagent kit. After following the procedure specified by the supplier, cDNA samples are obtained and can be stored at -20ºC until further use.

qPCR

For PCR amplification and detection 384-well PCR microplates (Corning) are used. 20 ng of cDNA are loaded into each of the wells, as well as a cDNA negative

control. Furthermore, 2 µL of 5xPyroTaq EvaGreen qPCR Mix Plus (Cultek Molecular Bioline) are loaded into each of the wells. 0,2 µL of 1:10 diluted forward and reverse primers *(Table 4)* are added into each well, including target genes and two housekeeping genes. Plates are sealed, spun, and loaded into 480 II 96-well and 384-well plate LightCycler (Roche). Data are extracted using LightCycler 480 Software 1.5.

Table 4. **Primers used in qPCR.** Different primers used in quantitative PCR, as well as their target gene, sequence (Always forward, and reverse), and supplier.

Denomination	*Target Gene*	*Supplier*	*Sequence*
RFOL192	*FOSL2*	Sigma-Aldrich	ACAGTGATCACCTCCATGTCC
RFOL193			TGCCAATGGTCTTGATCACG
RFOL194	*FOSL1*		GATGAGAAATCTGGGCTGCAG
RFOL195			TTCCGGGATTTTGCAGATGG
RFOL208	*FOSB*		AAAAAGCAGAGCTGGAGTCG
RFOL209			TCTTCGTAGGGGATCTTGCAG
RFOL204	*FOS*		AGATTGCCAACCTGCTGAAG
RFOL205			AGCCACAGACATCTCTTCTGG
RFOL200	*JUN*		CTCCAAGTGCCGAAAAAGGAAG
RFOL201			GTTTAAGCTGTGCCACCTGTTC
RFOL126	*JUNB*		CTGGTGGCCTCTCTCTACACG
RFOL127			CCCGCGGGGGTAAAAGTACTG
RFOL210	*JUND*		AAGAGTCAGAACACGGAGCTG
RFOL211			TGACGTGGCTGAGGACTTTC
RFOL164	*GUSB*		GGAGCAGAAACGATTGCAGGG
RFOL165			TATTCCCCAGCACTCTCGTCG
RFOL146	*RPS26*		CTGCACTAACTGTGCCCGATGCGTG
RFOL147			GACGCTCGCTTCAGAAATGTCCCTG

Biostatistics

Three different experimental replicates were performed for each of the analyses. Statistical analysis was performed using GraphPad Prism 9.5.0. The method performed to compare the means of two or more datasets, as is the case, was an ordinary one or 2-way Analysis of Variance (ANOVA) with multiple comparisons between the means of every time point. Statistically significative comparisons with a 95 % or higher confidence are shown (P-values lower than 0,05).

References

Al-khayyat, W., Pirkkanen, J., Dougherty, J., Laframboise, T., Dickinson, N., Khaper, N., Lees, S. J., Mendonca, M. S., Boreham, D. R., Tai, T. C., Thome, C., & Tharmalingam, S. (2023). Overexpression of FRA1 (FOSL1) Leads to Global Transcriptional Perturbations, Reduced Cellular Adhesion and Altered Cell Cycle Progression. *Cells*, *12*(19). https://doi.org/10.3390/CELLS12192344/S1

Andrecht, S., Kolbus, A., Hartenstein, B., Angel, P., & Schorpp-Kistner, M. (2002). Cell cycle promoting activity of JunB through cyclin A activation. *Journal of Biological Chemistry*, *277*(39), 35961–35968. https://doi.org/10.1074/jbc.M202847200

Arnold, S., Kortland, J., Maltseva, D. V., Nersisyan, S. A., Samatov, T. R., Lezius, S., Tonevitsky, A. G., Milde-Langosch, K., Wicklein, D., Schumacher, U., & Stürken, C. (2022). Fra-2 overexpression upregulates pro-metastatic cell-adhesion molecules, promotes pulmonary metastasis, and reduces survival in a spontaneous xenograft model of human breast cancer. *Journal of Cancer Research and Clinical Oncology*, *148*(6), 1525–1542. https://doi.org/10.1007/s00432-021-03812-2

Bai, Y., Lv, Y. N., Zeng, M., Jia, P. Y., Lu, H. N., Zhu, Y. B., Li, S., Cui, Y. Y., & Luan, Y. X. (2020). Selection of Reference Genes for Normalization of Gene Expression in Thermobia domestica (Insecta: Zygentoma: Lepismatidae). *Genes*, *12*(1), 1–14. https://doi.org/10.3390/GENES12010021

Bakiri, L., Lallemand, D., Bossy-Wetzel, E., & Yaniv, M. (2000). Cell cycle-dependent variations in c-Jun and JunB phosphorylation: a role in the control of cyclin D1 expression. *The EMBO Journal*, *19*(9), 2056–2068. https://doi.org/10.1093/EMBOJ/19.9.2056

Bamberger, A. M., Milde-Langosch, K., Rössing, E., Goemann, C., & Löning, T. (2001). Expression pattern of the AP-1 family in endometrial cancer: Correlations with cell cycle regulators. *Journal of Cancer Research and Clinical Oncology*, *127*(9), 545–550. https://doi.org/10.1007/s004320100255

Bejjani, F., Evanno, E., Zibara, K., Piechaczyk, M., & Jariel-Encontre, I. (2019). The AP-1 transcriptional complex: Local switch or remote command? In *Biochimica et Biophysica Acta - Reviews on Cancer* (Vol. 1872, Issue 1, pp. 11–23). Elsevier B.V. https://doi.org/10.1016/j.bbcan.2019.04.003

Botes, M., De Kwaadsteniet, M., & Cloete, T. E. (2012). Application of quantitative PCR for the detection of microorganisms in water. *Analytical and Bioanalytical Chemistry 2012 405:1*, *405*(1), 91–108. https://doi.org/10.1007/S00216-012-6399-3

Bray, F., Ferlay, J., Soerjomataram, I., Siegel, R. L., Torre, L. A., & Jemal, A. (2018). Global cancer statistics 2018: GLOBOCAN estimates of incidence and mortality worldwide for 36 cancers in 185 countries. *CA: A Cancer Journal for Clinicians*, *68*(6), 394–424. https://doi.org/10.3322/caac.21492

Brown, J. R., Nigh, E., Lee, R. J., Ye, H., Thompson, M. A., Saudou, F., Pestell, R. G., & Greenberg, M. E. (1998). Fos family members induce cell cycle entry by activating cyclin D1. *Molecular and Cellular Biology*, *18*(9), 5609–5619. https://doi.org/10.1128/MCB.18.9.5609

Brüsselbach, S., Möhle-Steinlein, U., Wang, Z., Schreiber, M., Lucibello, F. C., Müller, R., & Wagner, E. (1995). Cell proliferation and cell cycle progression are not impaired in fibroblasts and ES cells lacking c-Fos. *Oncogene*.

Carrera, P. M., & Ormond, M. (2015). Current practice in and considerations for personalized medicine in lung cancer: From the patient's molecular biology to patient values and preferences. In *Maturitas* (Vol. 82, Issue 1, pp. 94–99). Elsevier Ireland Ltd. https://doi.org/10.1016/j.maturitas.2015.04.008

Casalino, L., Bakiri, L., Talotta, F., Weitzman, J. B., Fusco, A., Yaniv, M., & Verde, P. (2007). Fra-1 promotes growth and survival in RAS-transformed thyroid cells by controlling cyclin A transcription. *The EMBO Journal*, *26*(7), 1878–1890. https://doi.org/10.1038/SJ.EMBOJ.7601617

Chen, G. L., Li, R., Chen, X. X., Wang, J., Cao, S., Song, R., Zhao, M. C., Li, L. M., Hannemmann, N., Schett, G., Qian, C., & Bozec, A. (2021). Fra-2/AP-1 regulates melanoma cell metastasis by downregulating Fam212b. *Cell Death and Differentiation*, *28*(4), 1364–1378. https://doi.org/10.1038/s41418-020-00660-4

Chen, H., Wang, L., Liu, J., Wan, Z., Zhou, L., Liao, H., & Wan, R. (2023). LncRNA ITGB2-AS1 promotes cisplatin resistance of non-small cell lung cancer by inhibiting ferroptosis via activating the FOSL2/NAMPT axis. *Cancer Biology & Therapy*, *24*(1). https://doi.org/10.1080/15384047.2023.2223377

Chevallier, M., Borgeaud, M., Addeo, A., & Friedlaender, A. (2021). Oncogenic driver mutations in non-small cell lung cancer: Past, present and future. *World Journal of Clinical Oncology*, *12*(4), 217–237. https://doi.org/10.5306/wjco.v12.i4.217

Crowe, D. L., Brown, T. N., Kim, R., Smith, S. M., & Lee, M. K. (2000). A c-fos/estrogen receptor fusion protein promotes cell cycle progression and proliferation of human cancer cell lines. *Molecular Cell Biology Research Communications*, *3*(4), 243–248. https://doi.org/10.1006/mcbr.2000.0221

Curtis Bird, R. C., Tzeng Kung, T. Y. T., Wu, G., & Young-White, R. R. (1990). Variations in c-fos mRNA expression during serum induction and the synchronous cell cycle. *Biochemistry and Cell Biology = Biochimie et Biologie Cellulaire*, *68*(5), 858–862. https://doi.org/10.1139/O90-127

da Costa-Nunes, J. A., Gierlinski, M., Sasaki, T., Haagensen, E. J., Gilbert, D. M., & Blow, J. J. (2023). The location and development of Replicon Cluster Domains in early replicating DNA. *Wellcome Open Research*, *8*. https://doi.org/10.12688/WELLCOMEOPENRES.18742.2

Davis, P. K., Ho, A., & Dowdy, S. F. (2001). Biological methods for cell-cycle synchronization of mammalian cells. *BioTechniques*, *30*(6), 1322–1331. https://doi.org/10.2144/01306RV01

Deb, D., Moore, A. C., & Roy, U. B. (2022). The 2021 Global Lung Cancer Therapy Landscape. *Journal of Thoracic Oncology*, *17*(7), 931–936. https://doi.org/10.1016/j.jtho.2022.03.018

Dobrzanski, P., Noguchi, T., Kovary, K., Rizzo, C. A., Lazo, P. S., & Bravo, R. (1991). Both products of the fosB gene, FosB and its short form, FosB/SF, are transcriptional activators in fibroblasts. *Molecular and Cellular Biology*, *11*(11), 5470–5478. https://doi.org/10.1128/MCB.11.11.5470-5478.1991

Dong, X., Yang, Q., Du, Z., Zhang, G., Shi, C., Qin, X., & Song, Y. (2022). Identification of optimal reference genes for gene expression normalization in human osteosarcoma cell lines under proliferative conditions. *Frontiers in Genetics*, *13*. https://doi.org/10.3389/FGENE.2022.989990

Eferl, R., Ricci, R., Kenner, L., Zenz, R., David, J. P., Rath, M., & Wagner, E. F. (2003). Liver tumor development: c-Jun antagonizes the proapoptotic activity of p53. *Cell*, *112*(2), 181–192. https://doi.org/10.1016/S0092-8674(03)00042-4

Eferl, R., & Wagner, E. F. (2003). AP-1: a double-edged sword in tumorigenesis. *Nature Reviews. Cancer*, *3*(11), 859–868. https://doi.org/10.1038/NRC1209

Elliott, B., Millena, A. C., Matyunina, L., Zhang, M., Zou, J., Wang, G., Zhang, Q., Bowen, N., Eaton, V., Webb, G., Thompson, S., McDonald, J., & Khan, S. (2019). Essential role of JunD in cell proliferation is mediated via MYC signaling in prostate cancer cells. *Cancer Letters*, *448*, 155–167. https://doi.org/10.1016/J.CANLET.2019.02.005

Englert, C., Hou, X., Maheswaran, S., Bennett, P., Ngwu, C., Re, G. G., Garvin, A. J., Rosner, M. R., & Haber, D. A. (1995). WT1 suppresses synthesis of the epidermal growth factor receptor and induces apoptosis. *The EMBO Journal*, *14*(19), 4662. https://doi.org/10.1002/J.1460-2075.1995.TB00148.X

Farràs, R., Baldin, V., Gallach, S., Acquaviva, C., Bossis, G., Jariel-Encontre, I., & Piechaczyk, M. (2008). JunB breakdown in mid-/late G2 is required for down-regulation of cyclin A2 levels and proper mitosis. *Molecular and Cellular Biology*, *28*(12), 4173–4187. https://doi.org/10.1128/MCB.01620-07

Feng, X., Guan, N., Xu, E., Miao, Y., & Li, C. (2021). Transcription Factors Leading to High Expression of Neuropeptide L1CAM in Brain Metastases from Lung Adenocarcinoma and Clinical Prognostic Analysis. *Disease Markers*, *2021*. https://doi.org/10.1155/2021/8585633

Gao, F., Li, M., Zhou, L., Liu, W., Zuo, H., & Li, W. (2020). Xanthohumol targets the ERK1/2-Fra1 signaling axis to reduce cyclin D1 expression and inhibit non-small cell lung cancer. *Oncology Reports*, *44*(4), 1365–1374. https://doi.org/10.3892/OR.2020.7697

Glover, J. N. M., & Harrison, S. C. (1995). Crystal structure of the heterodimeric bZIP transcription factor c-Fos-c-Jun bound to DNA. *NATURE*, 257–261.

Günthert, A. R., Gründker, C., Hollmann, K., & Emons, G. (2002). Luteinizing hormone-releasing hormone induces JunD-DNA binding and extends cell cycle in human

ovarian cancer cells. *Biochemical and Biophysical Research Communications*, *294*(1), 11–15. https://doi.org/10.1016/S0006-291X(02)00427-8

Halazonetis, T. D., Georgopoulos, K., Greenberg, M. E., & Leder, P. (1988). c-Jun dimerizes with itself and with c-Fos, forming complexes of different DNA binding affinities. *Cell*, *55*(5), 917–924. https://doi.org/10.1016/0092-8674(88)90147-X

Hanahan, D. (2022). Hallmarks of Cancer: New Dimensions. In *Cancer Discovery* (Vol. 12, Issue 1, pp. 31–46). American Association for Cancer Research Inc. https://doi.org/10.1158/2159-8290.CD-21-1059

Hanahan, D., & Weinberg, R. A. (2011). Hallmarks of cancer: The next generation. In *Cell* (Vol. 144, Issue 5, pp. 646–674). https://doi.org/10.1016/j.cell.2011.02.013

He, L., Sneider, A., Chen, W., Karl, M., Prasath, V., Wu, P. H., Mattson, G., & Wirtz, D. (2017). Mammalian Cell Division in 3D Matrices via Quantitative Confocal Reflection Microscopy. *Journal of Visualized Experiments : JoVE*, *2017*(129), 56364. https://doi.org/10.3791/56364

Kamide, D., Yamashita, T., Araki, K., Tomifuji, M., Tanaka, Y., Tanaka, S., Shiozawa, S., & Shiotani, A. (2016). Selective activator protein-1 inhibitor T-5224 prevents lymph node metastasis in an oral cancer model. *Cancer Science*, *107*(5), 666–673. https://doi.org/10.1111/CAS.12914

Khan, F. I., Shahbaaz, M., Bisetty, K., Waheed, A., Sly, W. S., Ahmad, F., & Hassan, M. I. (2016). Large scale analysis of the mutational landscape in β-glucuronidase: A major player of mucopolysaccharidosis type VII. *Gene*, *576*(1 Pt 1), 36–44. https://doi.org/10.1016/J.GENE.2015.09.062

Lamouille, S., Xu, J., & Derynck, R. (2014). Molecular mechanisms of epithelial-mesenchymal transition. In *Nature Reviews Molecular Cell Biology* (Vol. 15, Issue 3, pp. 178–196). https://doi.org/10.1038/nrm3758

Li, J., Zhou, L., Jiang, H., Lin, L., & Li, Y. (2022). Inhibition of FOSL2 aggravates the apoptosis of ovarian cancer cells by promoting the formation of inflammasomes. *Genes & Genomics*, *44*(1), 29–38. https://doi.org/10.1007/S13258-021-01152-6

Li, L., Jiang, H., Zeng, B., Wang, X., Bao, Y., Chen, C., Ma, L., & Yuan, J. (2024). Liquid biopsy in lung cancer. *Clinica Chimica Acta; International Journal of Clinical Chemistry*, *554*, 117757. https://doi.org/10.1016/j.cca.2023.117757

Li, Y., Yan, B., & He, S. (2023). Advances and challenges in the treatment of lung cancer. In *Biomedicine and Pharmacotherapy* (Vol. 169). Elsevier Masson s.r.l. https://doi.org/10.1016/j.biopha.2023.115891

Luo, L., Chi, H., & Ling, J. (2018). MiR-124-3p suppresses glioma aggressiveness via targeting of Fra-2. *Pathology, Research and Practice*, *214*(11), 1825–1834. https://doi.org/10.1016/J.PRP.2018.09.017

Malhotra, J., Malvezzi, M., Negri, E., La Vecchia, C., & Boffetta, P. (2016). Risk factors for lung cancer worldwide. *European Respiratory Journal*, *48*(3), 889–902. https://doi.org/10.1183/13993003.00359-2016

Manoir, S. Du, Guillaud, P., Camus, E., Seigneurin, D., & Brugal, G. (1991). Ki-67 labeling in postmitotic cells defines different Ki-67 pathways within the 2c compartment. *Cytometry*, *12*(5), 455–463. https://doi.org/10.1002/CYTO.990120511

Martínez-Alonso, D., & Malumbres, M. (2020). Mammalian cell cycle cyclins. *Seminars in Cell & Developmental Biology*, *107*, 28–35. https://doi.org/10.1016/J.SEMCDB.2020.03.009

Medema, R. H., Klompmaker, R., Smits, V. A. J., & Rijksen, G. (1998). p21waf1 can block cells at two points in the cell cycle, but does not interfere with processive DNA-replication or stress-activated kinases. *Oncogene*, *16*(4), 431–441. https://doi.org/10.1038/SJ.ONC.1201558

Motomura, H., Seki, S., Shiozawa, S., Aikawa, Y., Nogami, M., & Kimura, T. (2018). A selective c-Fos/AP-1 inhibitor prevents cartilage destruction and subsequent osteophyte formation. *Biochemical and Biophysical Research Communications*, *497*(2), 756–761. https://doi.org/10.1016/J.BBRC.2018.02.147

Nicholson, A. G., Tsao, M. S., Beasley, M. B., Borczuk, A. C., Brambilla, E., Cooper, W. A., Dacic, S., Jain, D., Kerr, K. M., Lantuejoul, S., Noguchi, M., Papotti, M., Rekhtman, N., Scagliotti, G., van Schil, P., Sholl, L., Yatabe, Y., Yoshida, A., & Travis, W. D. (2022). The 2021 WHO Classification of Lung Tumors: Impact of Advances Since 2015. In *Journal of Thoracic Oncology* (Vol. 17, Issue 3, pp. 362–387). Elsevier Inc. https://doi.org/10.1016/j.jtho.2021.11.003

Njouendou, A. J., Szarvas, T., Tiofack, A. A. Z., Kenfack, R. N., Tonouo, P. D., Ananga, S. N., Bell, E. H. M. D., Simo, G., Hoheisel, J. D., Siveke, J. T., & Lueong, S. S. (2023). SOX2 dosage sustains tumor-promoting inflammation to drive disease aggressiveness by modulating the FOSL2/IL6 axis. *Molecular Cancer*, *22*(1). https://doi.org/10.1186/S12943-023-01734-W

Nowak, C. M., Quarton, T., & Bleris, L. (2023). Impact of variability in cell cycle periodicity on cell population dynamics. *PLOS Computational Biology*, *19*(6), e1011080. https://doi.org/10.1371/JOURNAL.PCBI.1011080

Oh, E. T., Kim, H. G., Kim, C. H., Lee, J., Kim, C., Lee, J. S., Cho, Y., & Park, H. J. (2023). NQO1 regulates cell cycle progression at the G2/M phase. *Theranostics*, *13*(3), 873–895. https://doi.org/10.7150/THNO.77444

Okada, S., Fukuda, T., Inada, K., & Tokuhisa, T. (1999). Prolonged Expression of c-fos Suppresses Cell Cycle Entry of Dormant Hematopoietic Stem Cells. *Blood*, *93*(3), 816–825. https://doi.org/10.1182/BLOOD.V93.3.816

Pai, S., & Bird, R. C. (1994). c-fos expression is required during all phases of the cell cycle during exponential cell proliferation. *Anticancer Research*.

Passegué, E., & Wagner, E. F. (2000). JunB suppresses cell proliferation by transcriptional activation of p16(INK4a) expression. *The EMBO Journal*, *19*(12), 2969–2979. https://doi.org/10.1093/EMBOJ/19.12.2969

Pérez-Benavente, B., & Farràs, R. (2016). Cell Synchronization Techniques to Study the Action of CDK Inhibitors. *Methods in Molecular Biology (Clifton, N.J.)*, *1336*, 85–93. https://doi.org/10.1007/978-1-4939-2926-9_8

Pérez-Benavente, B., Fathinajafabadi, A., de la Fuente, L., Gandía, C., Martínez-Férriz, A., Pardo-Sánchez, J. M., Milián, L., Conesa, A., Romero, O. A., Carretero, J., Matthiesen, R., Jariel-Encontre, I., Piechaczyk, M., & Farràs, R. (2022). New roles for AP-1/JUNB in cell cycle control and tumorigenic cell invasion via regulation of cyclin E1 and TGF-β2. *Genome Biology*, *23*(1). https://doi.org/10.1186/S13059-022-02800-0

Rampioni Vinciguerra, G. L., Capece, M., Scafetta, G., Rentsch, S., Vecchione, A., Lovat, F., & Croce, C. M. (2023). Role of Fra-2 in cancer. In *Cell Death and Differentiation*. Springer Nature. https://doi.org/10.1038/s41418-023-01248-4

Razavi, S. A., Afsharpad, M., Modarressi, M. H., Zarkesh, M., Yaghmaei, P., Nasiri, S., Tavangar, S. M., Gholami, H., Daneshafrooz, A., & Hedayati, M. (2019). Validation of Reference Genes for Normalization of Relative qRT-PCR Studies in Papillary Thyroid Carcinoma. *Scientific Reports*, *9*(1). https://doi.org/10.1038/S41598-019-49247-1

Rocco, G., Morabito, A., Leone, A., Muto, P., Fiore, F., & Budillon, A. (2016). Management of non-small cell lung cancer in the era of personalized medicine. In *International Journal of Biochemistry and Cell Biology* (Vol. 78, pp. 173–179). Elsevier Ltd. https://doi.org/10.1016/j.biocel.2016.07.011

Sarode, P., Zheng, X., Giotopoulou, G. A., Giotopoulou, G. A., Weigert, A., Kuenne, C., Günther, S., Friedrich, A., Gattenlöhner, S., Stiewe, T., Brüne, B., Brüne, B., Grimminger, F., Stathopoulos, G. T., Stathopoulos, G. T., Pullamsetti, S. S., Pullamsetti, S. S., Seeger, W., Seeger, W., … Savai, R. (2020). Reprogramming of tumor-associated macrophages by targeting β-catenin/FOSL2/ARID5A signaling: A potential treatment of lung cancer. *Science Advances*, *6*(23). https://doi.org/10.1126/SCIADV.AAZ6105

Shaulian, E., & Karin, M. (2002). AP-1 as a regulator of cell life and death. In *NATURE CELL BIOLOGY* (Vol. 4). http://cellbio.nature.comE131

Singh, K. K., Gupta, A., Bharti, C., & Sharma, H. (2021). Emerging techniques of western blotting for purification and analysis of protein. *Future Journal of Pharmaceutical Sciences 2021 7:1*, *7*(1), 1–14. https://doi.org/10.1186/S43094-021-00386-1

Smith, C. J., & Osborn, A. M. (2009). Advantages and limitations of quantitative PCR (Q-PCR)-based approaches in microbial ecology. *FEMS Microbiology Ecology*, *67*(1), 6–20. https://doi.org/10.1111/J.1574-6941.2008.00629.X

Song, D., Lian, Y., & Zhang, L. (2023). The potential of activator protein 1 (AP-1) in cancer targeted therapy. In *Frontiers in Immunology* (Vol. 14). Frontiers Media SA. https://doi.org/10.3389/fimmu.2023.1224892

Sunters, A., Mccluskey, J., & Grigoriadis, A. E. (1998). Control of Cell Cycle Gene Expression in Bone Development and During c-Fos-Induced Osteosarcoma

Formation. *Dev. Genet*, *22*, 386–397. https://doi.org/10.1002/(SICI)1520-6408(1998)22:4

Sunters, A., Thomas, D. P., Yeudall, W. A., & Grigoriadis, A. E. (2004). Accelerated cell cycle progression in osteoblasts overexpressing the c-fos proto-oncogene: induction of cyclin A and enhanced CDK2 activity. *The Journal of Biological Chemistry*, *279*(11), 9882–9891. https://doi.org/10.1074/JBC.M310184200

Swanton, C., Bernard, E., Abbosh, C., André, F., Auwerx, J., Balmain, A., Bar-Sagi, D., Bernards, R., Bullman, S., DeGregori, J., Elliott, C., Erez, A., Evan, G., Febbraio, M. A., Hidalgo, A., Jamal-Hanjani, M., Joyce, J. A., Kaiser, M., Lamia, K., … Hanahan, D. (2024). Embracing cancer complexity: Hallmarks of systemic disease. In *Cell* (Vol. 187, Issue 7, pp. 1589–1616). Elsevier B.V. https://doi.org/10.1016/j.cell.2024.02.009

Tie, L., Xiao, H., Wu, D., Yang, Y., & Wang, P. (2020). *A brief guide to good practices in pharmacological experiments: Western blotting*. https://doi.org/10.1038/s41401-020-00539-7

Trop-Steinberg, S., & Azar, Y. (2017). AP-1 Expression and its Clinical Relevance in Immune Disorders and Cancer. *The American Journal of the Medical Sciences*, *353*(5), 474–483. https://doi.org/10.1016/J.AMJMS.2017.01.019

Verborg, W., Thomas, H., Bissett, D., Waterfall, J., Steiner, J., Cooper, M., & Rankin, E. M. (2007). First-into-man phase I and pharmacokinetic study of XR5944.14, a novel agent with a unique mechanism of action. *British Journal of Cancer 2007 97:7*, *97*(7), 844–850. https://doi.org/10.1038/sj.bjc.6603953

Vincent, S., Marty, L., & Fort, P. (1993). S26 ribosomal protein RNA: An invariant control for gene regulation experiments in eucaryotic cells and tissues. *Nucleic Acids Research*, *21*(6), 1498. https://doi.org/10.1093/NAR/21.6.1498

Vriz, S., Lemaitre, J.-M., Leibovici, M., Thierry, N., & Méchali, M. (1992). Comparative analysis of the intracellular localization of c-Myc, c-Fos, and replicative proteins during cell cycle progression. *Molecular and Cellular Biology*, *12*(8), 3548–3555. https://doi.org/10.1128/MCB.12.8.3548-3555.1992

Wan, X., Guan, S., Hou, Y., Qin, Y., Zeng, H., Yang, L., Qiao, Y., Liu, S., Li, Q., Jin, T., Qiu, Y., & Liu, M. (2021). FOSL2 promotes VEGF-independent angiogenesis by transcriptionnally activating Wnt5a in breast cancer-associated fibroblasts. *Theranostics*, *11*(10), 4975–4991. https://doi.org/10.7150/THNO.55074

Wang, J., An, F. S., Zhang, W., Gong, L., Wei, S. J., Qin, W. D., Wang, X. P., Zhao, Y. X., Zhang, Y., Zhang, C., & Zhang, M. X. (2011). Inhibition of c-Jun N-Terminal Kinase Attenuates Low Shear Stress-Induced Atherogenesis in Apolipoprotein E-Deficient Mice. *Molecular Medicine*, *17*(9–10), 990–999. https://doi.org/10.2119/MOLMED.2011.00073/FIGURES/7

Wang, J., Sun, D., Wang, Y., Ren, F., Pang, S., Wang, D., & Xu, S. (2014). FOSL2 positively regulates TGF-β1 signalling in non-small cell lung cancer. *PLoS ONE*, *9*(11). https://doi.org/10.1371/journal.pone.0112150

Wang, R. C., & Wang, Z. (2022). Synchronization of Cultured Cells to G1, S, G2, and M Phases by Double Thymidine Block. *Methods in Molecular Biology (Clifton, N.J.)*, *2579*, 61–71. https://doi.org/10.1007/978-1-0716-2736-5_5

Wang, Z. (2022). Cell Cycle Progression and Synchronization: An Overview. *Methods in Molecular Biology (Clifton, N.J.)*, *2579*, 3–23. https://doi.org/10.1007/978-1-0716-2736-5_1

Xu, K., Yin, X., Zhou, B., Zheng, X., Wang, H., Chen, J., Cai, X., Gao, H., Xu, X., Wang, L., Shen, L., Guo, T., Zheng, S., Li, B., Shao, Y., & Wang, J. (2023). FOSL2 promotes intertumoral infiltration of T cells and increases pathological complete response rates in locally advanced rectal cancer patients. *Cancer Letters*, *562*. https://doi.org/10.1016/J.CANLET.2023.216145

Zhang, Q., Adiseshaiah, P., & Reddy, S. P. (2005). Matrix metalloproteinase/epidermal growth factor receptor/mitogen-activated protein kinase signaling regulate fra-1 induction by cigarette smoke in lung epithelial cells. *American Journal of Respiratory Cell and Molecular Biology*, *32*(1), 72–81. https://doi.org/10.1165/RCMB.2004-0198OC

Zhang, S., Li, P., Li, J., Gao, J., Qi, Q., Dong, G., Liu, X., Jiao, Q., Wang, Y., Du, L., Zhan, H., Xu, S., & Wang, C. (2023). Chromatin accessibility uncovers KRAS-driven FOSL2 promoting pancreatic ductal adenocarcinoma progression through up-regulation of CCL28. *British Journal of Cancer*, *129*(3), 426–443. https://doi.org/10.1038/S41416-023-02313-Y

Zhang, X., Wu, J., Luo, S., Lechler, T., & Zhang, J. Y. (2016). FRA1 promotes squamous cell carcinoma growth and metastasis through distinct AKT and c-Jun dependent mechanisms. *Oncotarget*, *7*(23), 34371–34383. https://doi.org/10.18632/ONCOTARGET.9110

Zhang, Y., Vaccarella, S., Morgan, E., Li, M., Etxeberria, J., Chokunonga, E., Manraj, S. S., Kamate, B., Omonisi, A., & Bray, F. (2023). Global variations in lung cancer incidence by histological subtype in 2020: a population-based study. *The Lancet Oncology*, *24*(11), 1206–1218. https://doi.org/10.1016/S1470-2045(23)00444-8

Zhao, H. F., Wang, J., & To, S. S. T. (2015). The phosphatidylinositol 3-kinase/Akt and c-Jun N-terminal kinase signaling in cancer: Alliance or contradiction? (Review). *International Journal of Oncology*, *47*(2), 429–436. https://doi.org/10.3892/IJO.2015.3052

Annex

N1

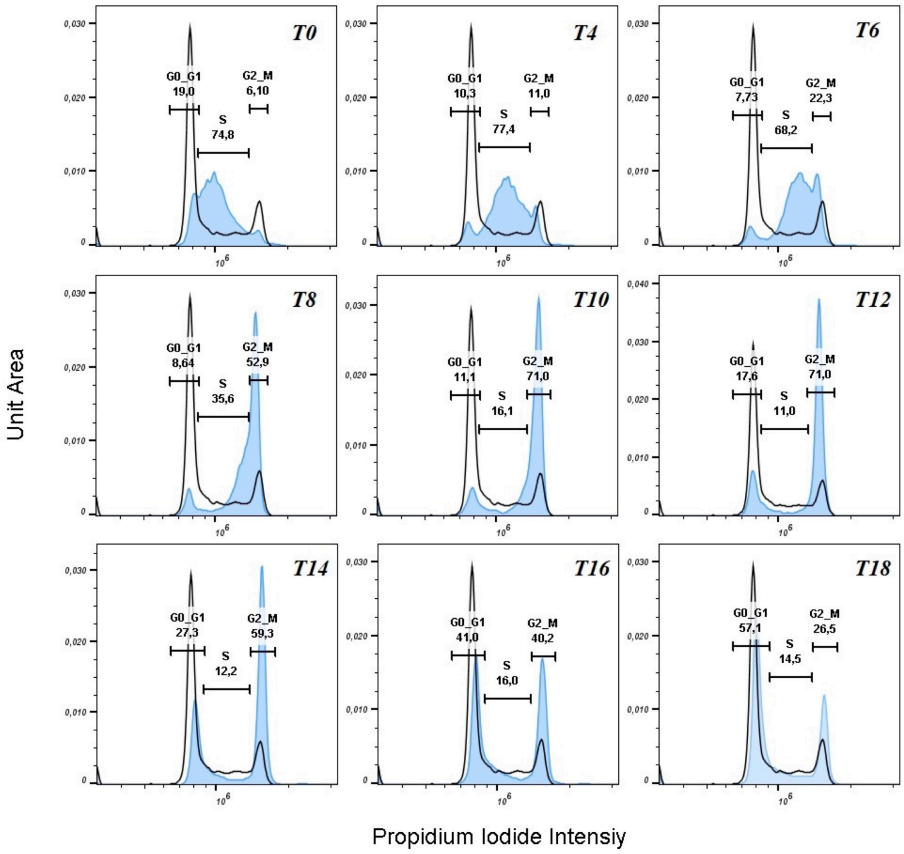
T0
G0_G1 19,0
G2_M 6,10
S 74,8
T4
G0_G1 10,3
G2_M 11,0
S 77,4
T6
G0_G1 7,73
G2_M 22,3
S 68,2
T8
G0_G1 8,64
G2_M 52,9
S 35,6
T10
G0_G1 11,1
G2_M 71,0
S 16,1
T12
G0_G1 17,6
G2_M 71,0
S 11,0
T14
G0_G1 27,3
G2_M 59,3
S 12,2
T16
G0_G1 41,0
G2_M 40,2
S 16,0
T18
G0_G1 57,1
G2_M 26,5
S 14,5
Unit Area
Propidium Iodide Intensiy

N2

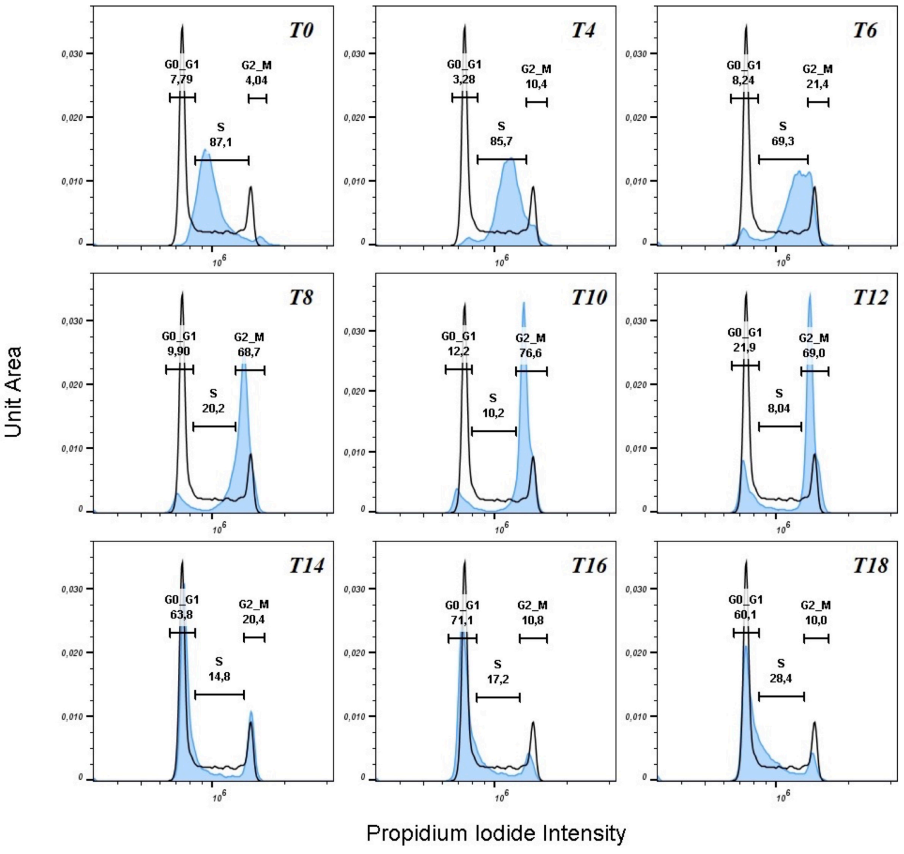
T0
G0_G1 7,79
G2_M 4,04
S 87,1
T4
G0_G1 3,28
G2_M 10,4
S 85,7
T6
G0_G1 8,24
G2_M 21,4
S 69,3
T8
G0_G1 9,90
G2_M 68,7
S 20,2
T10
G0_G1 12,2
G2_M 76,6
S 10,2
T12
G0_G1 21,9
G2_M 69,0
S 8,04
T14
G0_G1 63,8
G2_M 20,4
S 14,8
T16
G0_G1 71,1
G2_M 10,8
S 17,2
T18
G0_G1 60,1
G2_M 10,0
S 28,4
Unit Area
Propidium Iodide Intensity

A

N3

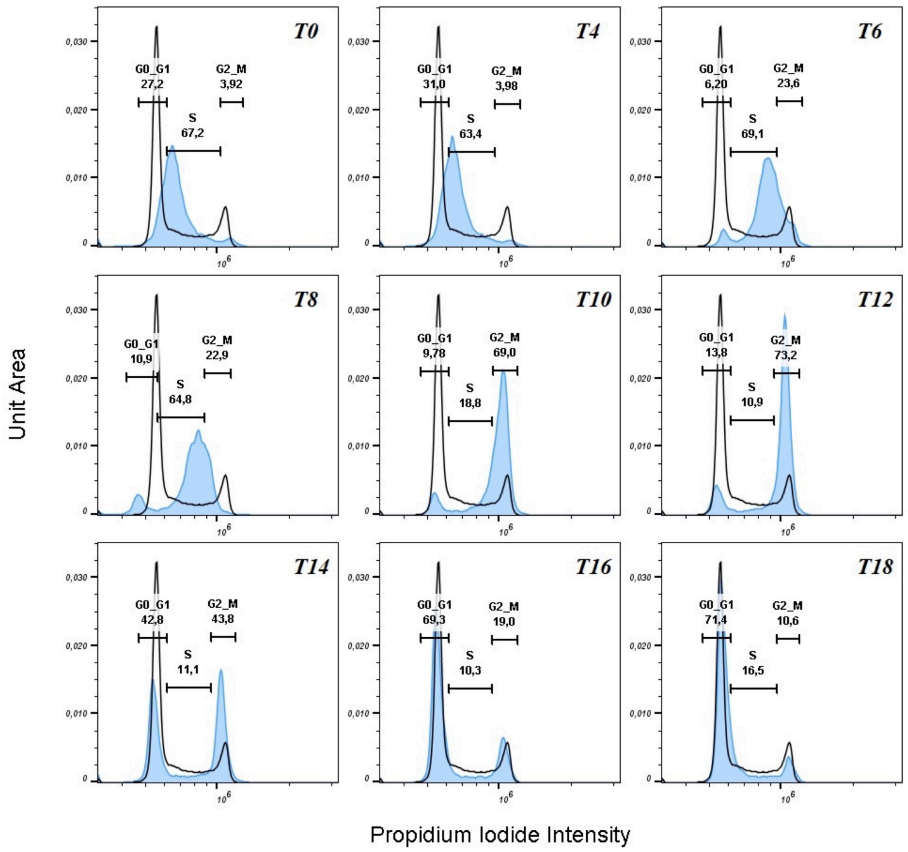

Annex Figure 1. **Genomic content variation across the cell cycle in osteosarcoma U2OS cells.** Histograms showing total DNA (X-axis) by propidium iodide staining and cell number (Unit Area) (Y-axis) across different times (h) after cell cycle release (T0-T18), as well as in a cell population with exponential growth (Overlay). Regions corresponding to G_0/G_1, S and G_2/M phases and their relative abundance are highlighted. Three experimental replicates shown. Data obtained using CytExpert Version 2.3 software. The flow cytometry results were analyzed using FlowJo™ v10.8 Software (BD Life Sciences).

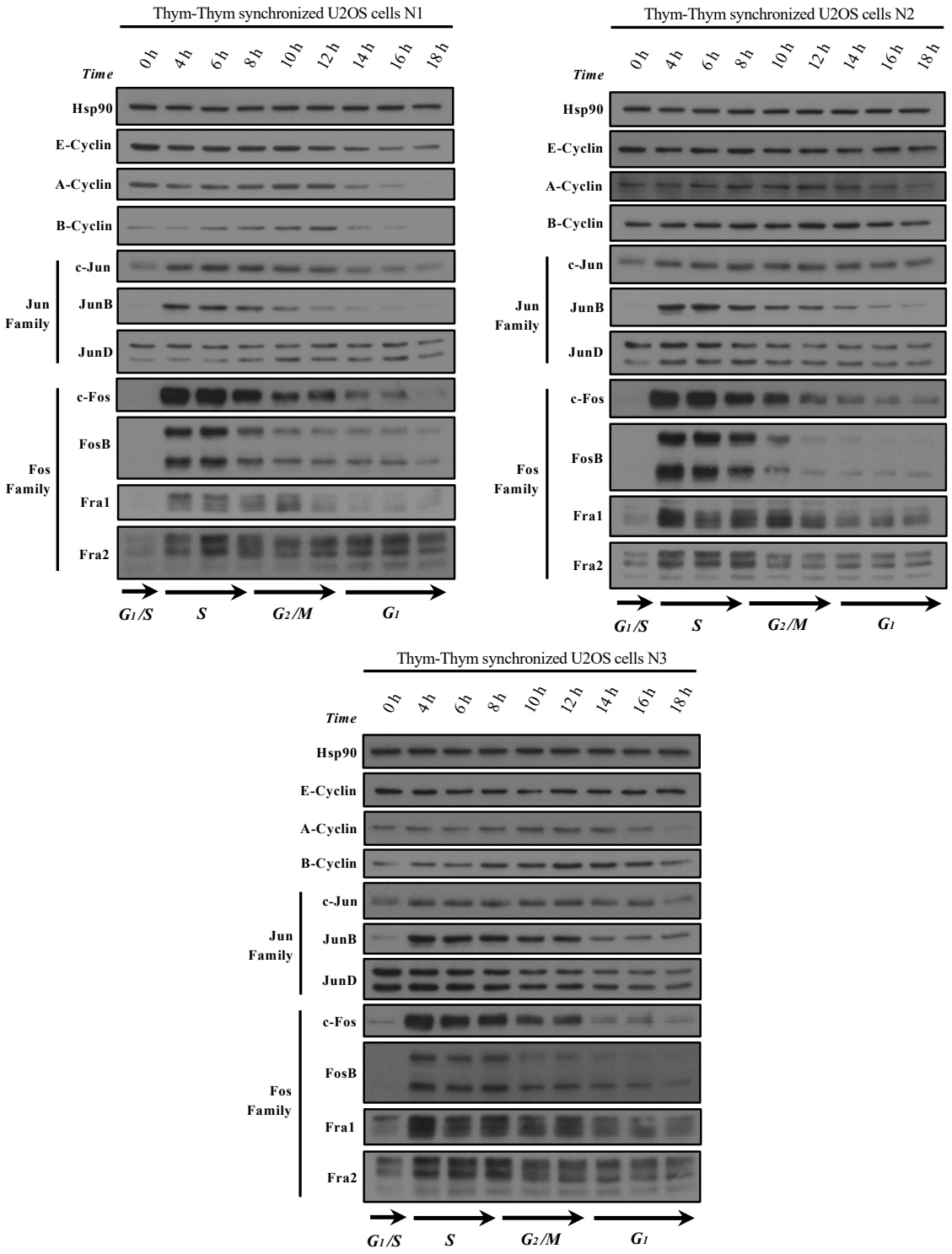

Annex Figure 2. **AP-1 protein level variation across the cell cycle in osteosarcoma U2OS cells (Raw Western Blot).** Osteosarcoma U2OS cells were assayed using WB at different times following cell cycle release by thymidine removal. Markers assayed included different representative cyclins, as well as all AP-1 (Jun and Fos) members and Hsp90 as a loading control. Three experimental replicates were performed.

Annex Table 1. **AP-1 protein level variation across the cell cycle in osteosarcoma U2OS cells.** WB was performed on U2OS osteosarcoma cells synchronized using double thymidine. Data is expressed as relative band intensity,

as fold ratio from values at 4 hours. Hsp90 was used as housekeeping gene for normalization. Three experimental replicates were performed. N1 from Fra2 was excluded from posterior analyses.

Relative band intensity (Fold change from T4)									
Target Gene	**c-Jun**			**JunB**			**JunD**		
Time after release (h)	N1	N2	N3	N1	N2	N3	N1	N2	N3
0	*0,407*	*0,473*	*0,674*	*0,015*	*0,021*	*0,093*	*0,765*	*0,528*	*0,963*
4	*1,000*	*1,000*	*1,000*	*1,000*	*1,000*	*1,000*	*1,000*	*1,000*	*1,000*
6	*1,198*	*0,921*	*1,065*	*0,891*	*0,873*	*1,005*	*0,818*	*0,782*	*0,955*
8	*1,057*	*1,005*	*1,042*	*0,664*	*0,548*	*0,908*	*0,911*	*0,634*	*0,830*
10	*0,933*	*0,995*	*0,988*	*0,340*	*0,393*	*0,690*	*1,180*	*0,524*	*0,690*
12	*0,894*	*1,057*	*1,102*	*0,173*	*0,341*	*0,677*	*1,344*	*0,426*	*0,684*
14	*0,520*	*0,855*	*0,787*	*0,077*	*0,190*	*0,295*	*1,077*	*0,440*	*0,538*
16	*0,429*	*0,785*	*1,026*	*0,057*	*0,102*	*0,314*	*1,468*	*0,384*	*0,579*
18	*0,362*	*0,693*	*0,449*	*0,013*	*0,034*	*0,274*	*0,902*	*0,346*	*0,402*

Relative band intensity (Fold change from T4)												
Target Gene	**c-Fos**			**FosB**			**Fra1**			**Fra2**		
Time after release (h)	N1	N2	N3	N1	N2	N3	N1	N2	N3	N1	N2	N3
0	0,008	0,011	0,057	0,006	0,003	0,021	0,048	0,093	0,305	*0,342*	0,245	0,422
4	1,000	1,000	1,000	1,000	1,000	1,000	1,000	1,000	1,000	*1,000*	1,000	1,000
6	0,911	0,875	0,939	0,920	0,831	0,831	0,929	0,562	0,795	*1,542*	0,875	1,129
8	0,725	0,651	0,879	0,494	0,577	0,864	0,807	0,655	0,915	*1,173*	0,871	1,084
10	0,420	0,519	0,571	0,332	0,222	0,424	0,973	0,712	0,760	*0,929*	0,472	0,851
12	0,462	0,306	0,575	0,239	0,065	0,513	0,422	0,490	0,866	*1,234*	0,433	0,827
14	0,173	0,208	0,169	0,224	0,031	0,335	0,168	0,264	0,568	*1,323*	0,451	0,676
16	0,170	0,135	0,253	0,214	0,027	0,310	0,193	0,321	0,508	*1,448*	0,446	0,823
18	0,038	0,091	0,097	0,114	0,030	0,155	0,138	0,308	0,376	*1,124*	0,392	0,558

Relative band intensity (Fold change from T4)									
Target Gene	**Cyclin A**			**Cyclin B**			**Cyclin E**		
Time after release (h)	N1	N2	N3	N1	N2	N3	N1	N2	N3
0	*1,348*	*0,975*	*0,942*	*1,080*	*0,745*	*0,629*	*1,165*	*0,966*	*1,188*
4	*1,000*	*1,000*	*1,000*	*1,000*	*1,000*	*1,000*	*1,000*	*1,000*	*1,000*
6	*1,154*	*1,086*	*1,031*	*2,256*	*1,070*	*1,084*	*0,983*	*0,987*	*0,979*
8	*1,143*	*1,159*	*1,334*	*2,893*	*1,166*	*1,708*	*0,950*	*0,936*	*1,071*
10	*1,466*	*1,299*	*1,827*	*3,472*	*1,085*	*1,743*	*0,901*	*0,828*	*0,736*

12	*1,434*	*1,696*	*1,660*	*4,780*	*1,313*	*2,267*	*0,721*	*0,940*	*0,973*
14	*0,529*	*0,988*	*1,505*	*1,219*	*1,192*	*2,056*	*0,487*	*0,759*	*0,894*
16	*0,210*	*0,857*	*1,063*	*0,666*	*0,944*	*2,063*	*0,316*	*1,013*	*1,167*
18	*0,034*	*0,400*	*0,255*	*0,000*	*0,746*	*0,994*	*0,432*	*0,772*	*1,102*

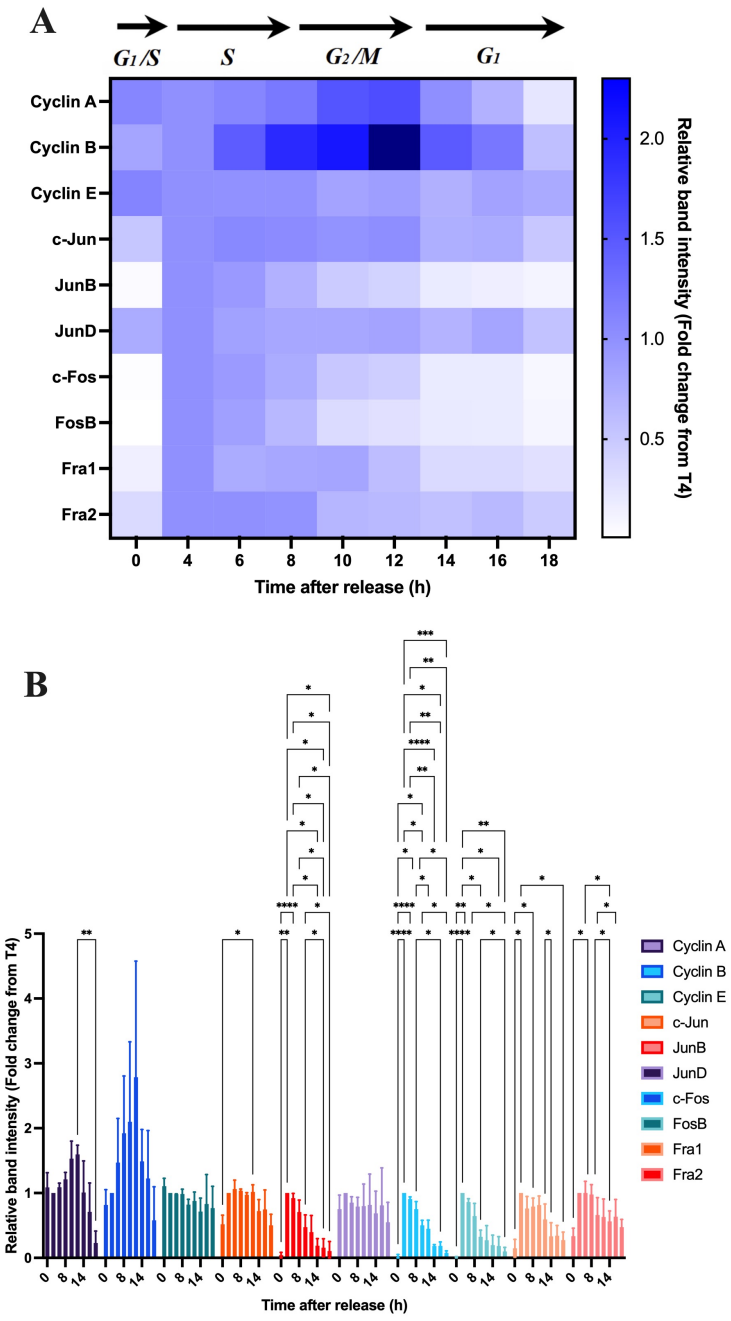

Annex Figure 3. **AP-1 protein level variation across the cell cycle in osteosarcoma U2OS cells.** Band intensity quantification was performed on WB from U2OS cells using Fiji (ImageJ). Absolute band intensity was normalized using the loading control. Afterwards, data was expressed as fold change from T4 (4 hours from release), and analysis was performed using GraphPad Prism 9.5.0. Ordinary 2-way ANOVA with multiple comparisons between the means of every time point. P-values inferior to 0,05 are represented. Three experimental replicates were performed. ***A.*** Heatmap representation of U2OS cells relative marker expression. ***B.*** Grouped column representation of U2OS cells relative marker expression.

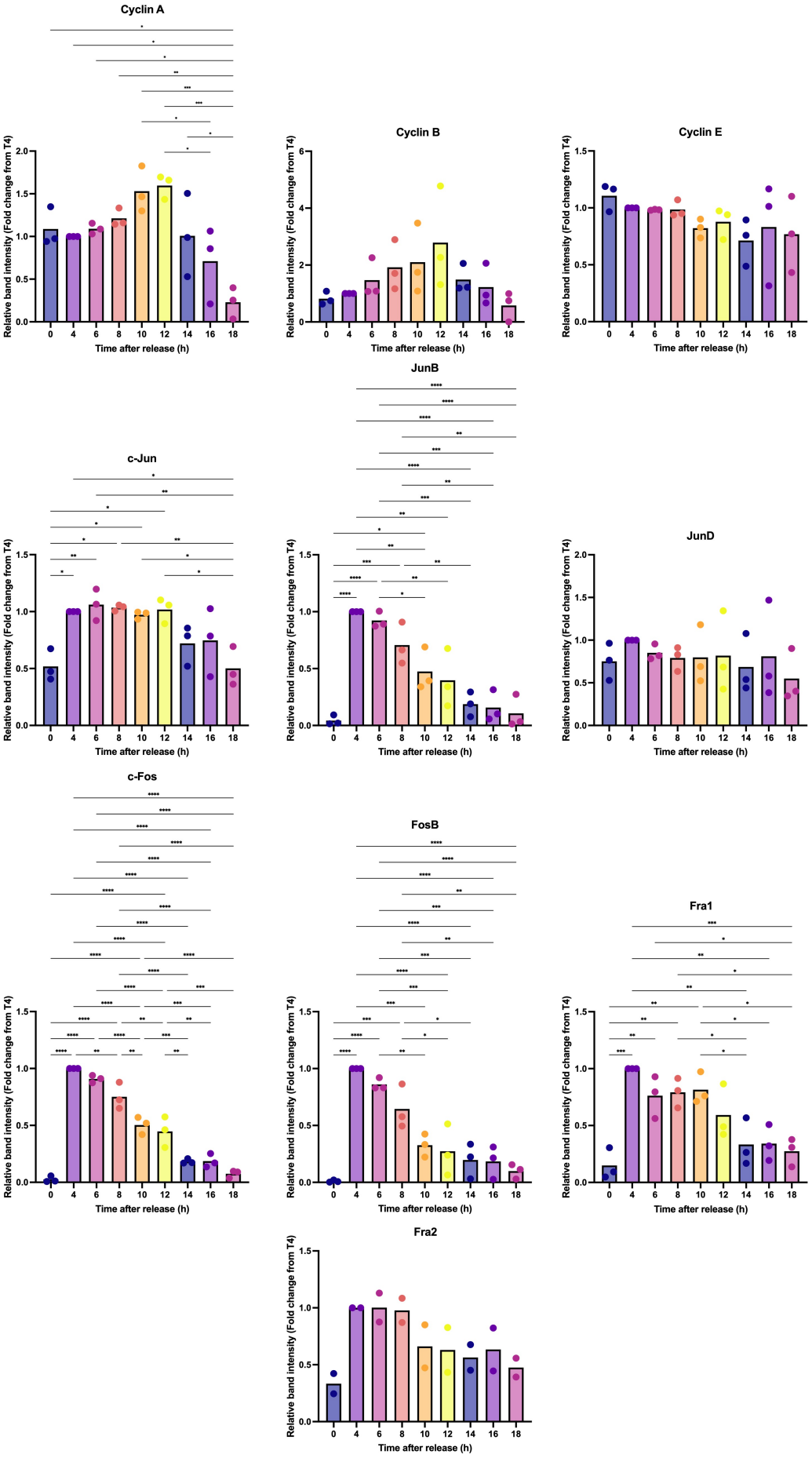
Cyclin A
Cyclin B
Cyclin E
JunB
c-Jun
JunD
c-Fos
FosB
Fra1
Fra2
Relative band intensity (Fold change from T4)
Time after release (h)

F

Annex Figure 4. **AP-1 protein level variation across the cell cycle in osteosarcoma U2OS cells (Individual representation).** Band intensity quantification was performed on WB from U2OS cells using Fiji (ImageJ). Absolute band intensity was normalized using the loading control. Afterwards, data was expressed as fold change from T4 (4 hours from release), and analysis was performed using GraphPad Prism 9.5.0. Ordinary one-way ANOVA with multiple comparisons between the means of every time point. P-values inferior to 0,05 are represented. Three experimental replicates were performed.

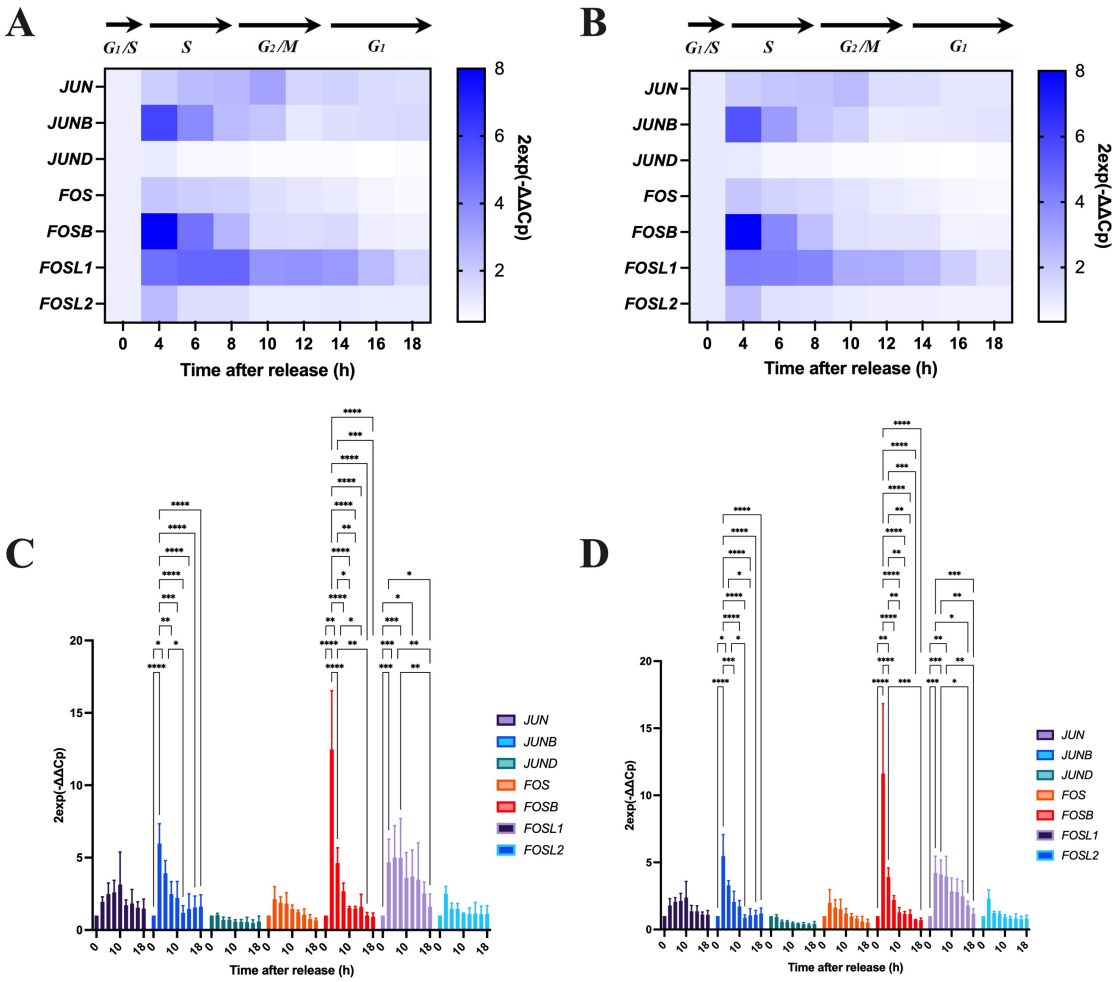

Annex Figure 5. **AP-1 mRNA level variation across the cell cycle in osteosarcoma U2OS cells.** RT-qPCR was performed on U2OS osteosarcoma cells synchronized using double-thymidine. Data is expressed as 2exp(-ΔΔCp), where Cp is the amplification cycle. Heatmap (***A*** and ***B***) and barplot (***C*** and ***D***) representation using *GUSB* (***A*** and ***C***) and *RPS26* (***B*** and ***D***) as housekeeping genes for normalization. Analysis was performed using GraphPad Prism 9.5.0. Ordinary 2-way ANOVA with multiple comparisons between the means of every time point. P-values inferior to 0,05 are represented. Three experimental replicates were performed.

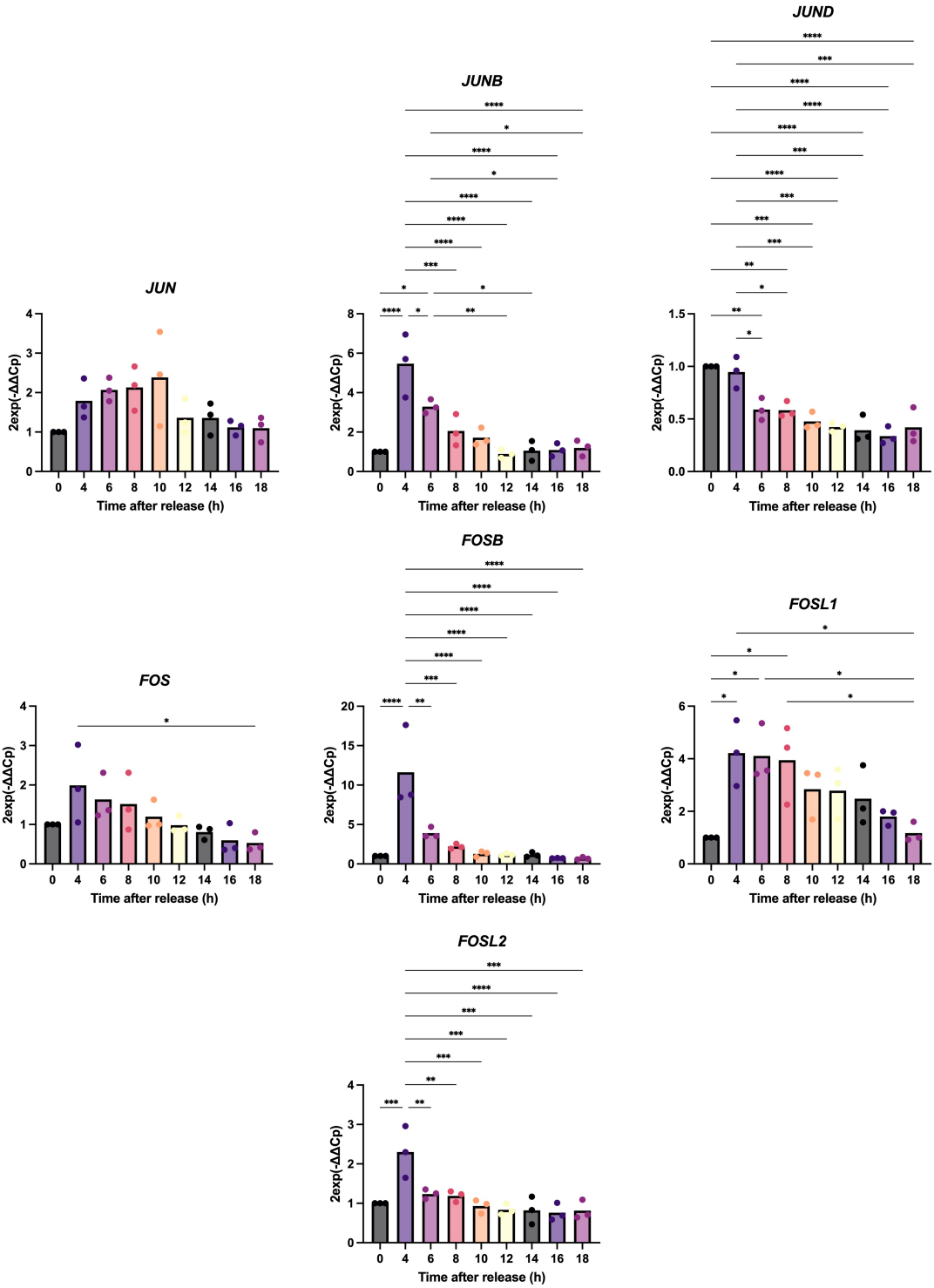

Annex Figure 6. **AP-1 mRNA level variation across the cell cycle in osteosarcoma U2OS cells (Individual representation).** RT-qPCR was performed on U2OS osteosarcoma cells synchronized using double-thymidine. Data is expressed as 2exp(-ΔΔCp), where Cp is the amplification cycle. Barplot representation using *RPS26* as housekeeping gene for normalization. Analysis was performed using GraphPad Prism 9.5.0. Ordinary one-way ANOVA with multiple comparisons between the means of every time point. P-values inferior to 0,05 are represented. Three experimental replicates were performed.

Annex Table 2. **AP-1 mRNA level variation across the cell cycle in osteosarcoma U2OS cells.** RT-qPCR was performed on U2OS osteosarcoma cells synchronized using double thymidine. Data is expressed as 2exp(-ΔΔCp), where Cp is the amplification cycle of detection. *GUSB* and *RPS26* were used as housekeeping genes for normalization. Three experimental replicates were performed.

2exp(-ΔΔCp)										
Target Gene		***JUN***			***JUNB***			***JUND***		
House-keeping Gene	***Time after release (h)***	N1	N2	N3	N1	N2	N3	N1	N2	N3
GUSB	0	*1*	*1*	*1*	*1*	*1*	*1*	*1*	*1*	*1*
	4	*2,29*	*1,96*	*1,59*	*6,76*	*6,76*	*4,38*	*1,06*	*1,14*	*0,92*
	6	*2,02*	*3,36*	*2,07*	*2,91*	*4,58*	*4,24*	*0,48*	*0,82*	*0,81*
	8	*2,73*	*3,36*	*1,71*	*2,99*	*2,96*	*1,48*	*0,55*	*0,84*	*0,74*
	10	*2,5*	*5,63*	*1,3*	*1,58*	*3,53*	*1,55*	*0,44*	*0,67*	*0,64*
	12	*1,86*	*1,99*	*1,3*	*0,89*	*1,76*	*0,9*	*0,38*	*0,73*	*0,55*
	14	*1,35*	*2,95*	*1,18*	*1,01*	*2,65*	*0,7*	*0,29*	*0,92*	*0,43*
	16	*1,39*	*2*	*1,25*	*1,16*	*2,47*	*1,04*	*0,33*	*0,74*	*0,38*
	18	*1,21*	*2,22*	*0,98*	*1,29*	*2,54*	*1*	*0,3*	*1*	*0,47*
RPS26	0	*1*	*1*	*1*	*1*	*1*	*1*	*1*	*1*	*1*
	4	*2,36*	*1,65*	*1,37*	*6,95*	*5,7*	*3,76*	*1,09*	*0,96*	*0,79*
	6	*2,05*	*2,38*	*1,78*	*2,96*	*3,25*	*3,66*	*0,49*	*0,58*	*0,7*
	8	*2,66*	*2,19*	*1,54*	*2,91*	*1,93*	*1,33*	*0,53*	*0,55*	*0,67*
	10	*2,46*	*3,54*	*1,15*	*1,55*	*2,22*	*1,37*	*0,44*	*0,42*	*0,57*
	12	*1,84*	*1,24*	*1*	*0,88*	*1,1*	*0,69*	*0,38*	*0,46*	*0,43*
	14	*1,44*	*1,72*	*0,91*	*1,08*	*1,54*	*0,54*	*0,31*	*0,54*	*0,33*
	16	*1,28*	*1,16*	*0,91*	*1,07*	*1,43*	*0,76*	*0,31*	*0,43*	*0,27*
	18	*1,19*	*1,36*	*0,74*	*1,27*	*1,56*	*0,76*	*0,29*	*0,61*	*0,36*

2exp(-ΔΔCp)													
Target Gene		***FOS***			***FOSB***			***FOSL1***			***FOSL2***		
House-keeeping Gene	***Time after release (h)***	N1	N2	N3	N1	N2	N3	N1	N2	N3	N1	N2	N3
GUSB	0	*1*	*1*	*1*	*1*	*1*	*1*	*1*	*1*	*1*	*1*	*1*	*1*
	4	*2,93*	*2,26*	*1,22*	*17,15*	*10,42*	*9,85*	*4,11*	*6,48*	*3,44*	*2,87*	*2,73*	*1,93*
	6	*2,28*	*1,92*	*1,43*	*3,45*	*4,98*	*5,45*	*3,49*	*7,55*	*3,96*	*1,23*	*1,91*	*1,29*
	8	*2,38*	*2,11*	*0,97*	*2,63*	*3,26*	*2,15*	*4,54*	*7,89*	*2,51*	*1,33*	*1,88*	*1,15*
	10	*1,66*	*1,54*	*1,13*	*1,59*	*1,4*	*1,58*	*3,51*	*5,39*	*1,91*	*1,09*	*1,18*	*1,11*
	12	*1,23*	*1,37*	*1,13*	*1,38*	*1,65*	*1,45*	*3,1*	*5,75*	*2,23*	*0,81*	*1,59*	*0,94*
	14	*0,88*	*1,5*	*0,78*	*0,85*	*2,56*	*1,37*	*1,98*	*6,42*	*2,03*	*0,78*	*2,01*	*0,61*
	16	*1,11*	*0,61*	*0,55*	*0,8*	*1,2*	*1,03*	*2,12*	*3,44*	*1,99*	*0,74*	*1,73*	*0,81*

	18	*0,82*	*0,61*	*0,55*	*0,66*	*0,94*	*1,16*	*0,94*	*2,6*	*1,31*	*0,73*	*1,77*	*0,84*
RPS26	0	*1*	*1*	*1*	*1*	*1*	*1*	*1*	*1*	*1*	*1*	*1*	*1*
	4	*3,02*	*1,9*	*1,05*	*17,63*	*8,78*	*8,46*	*4,23*	*5,46*	*2,96*	*2,96*	*2,3*	*1,65*
	6	*2,31*	*1,36*	*1,23*	*3,51*	*3,53*	*4,7*	*3,55*	*5,35*	*3,42*	*1,25*	*1,35*	*1,11*
	8	*2,31*	*1,38*	*0,87*	*2,56*	*2,13*	*1,93*	*4,42*	*5,16*	*2,26*	*1,3*	*1,23*	*1,03*
	10	*1,63*	*0,97*	*1*	*1,57*	*0,88*	*1,39*	*3,45*	*3,39*	*1,69*	*1,07*	*0,74*	*0,98*
	12	*1,22*	*0,85*	*0,87*	*1,36*	*1,03*	*1,11*	*3,07*	*3,59*	*1,71*	*0,8*	*0,99*	*0,72*
	14	*0,94*	*0,88*	*0,61*	*0,91*	*1,49*	*1,06*	*2,11*	*3,75*	*1,58*	*0,83*	*1,17*	*0,47*
	16	*1,03*	*0,36*	*0,4*	*0,73*	*0,7*	*0,75*	*1,95*	*2*	*1,45*	*0,69*	*1,01*	*0,59*
	18	*0,8*	*0,37*	*0,42*	*0,65*	*0,58*	*0,88*	*0,92*	*1,6*	*1*	*0,71*	*1,09*	*0,64*

Contribution to Sustainable Development Goals (2030 Agenda)

The present study, which aims to better understand the molecular basis of cancer, pathology which is expected to become the first global death cause in the following decades, is intimately linked with goal number 3 included in the Sustainable Development Goals or 2030 Agenda. This goal strives to ensure healthy lives and promote well-being for all at all ages. This objective has become remarkably important after the COVID-19 pandemic and calls for concerted efforts to achieve universal healthcare and sustainable financing for health, with special focus on environmental factors contributing to ill health. These environmental factors are key in cancer, with direct relationships between them and the onset of the pathology, as is the case with lung cancer and tobacco smoke, or UV exposure and skin cancer. There can be no universal and comprehensive healthcare without proper treatments for the diseases that hunt humanity, and no proper treatment will be developed without thorough research into the causes and molecular bases of pathologies. The present study will broaden the understanding of these molecular bases and contribute to better treat cancer patients in the future.